Chromosomal Translocation Formation Is Sufficient to Produce Fusion Circular RNAs Specific to Patient Tumor Cells

Loelia Babin, Marion Piganeau, Benjamin Renouf, Khadija Lamribet, Cécile Thirant, Ludovic Deriano, Thomas Mercher, Carine Giovannangeli, Erika Brunet

iScience

CellPress

Article

Chromosomal Translocation Formation Is Sufficient to Produce Fusion Circular RNAs Specific to Patient Tumor Cells

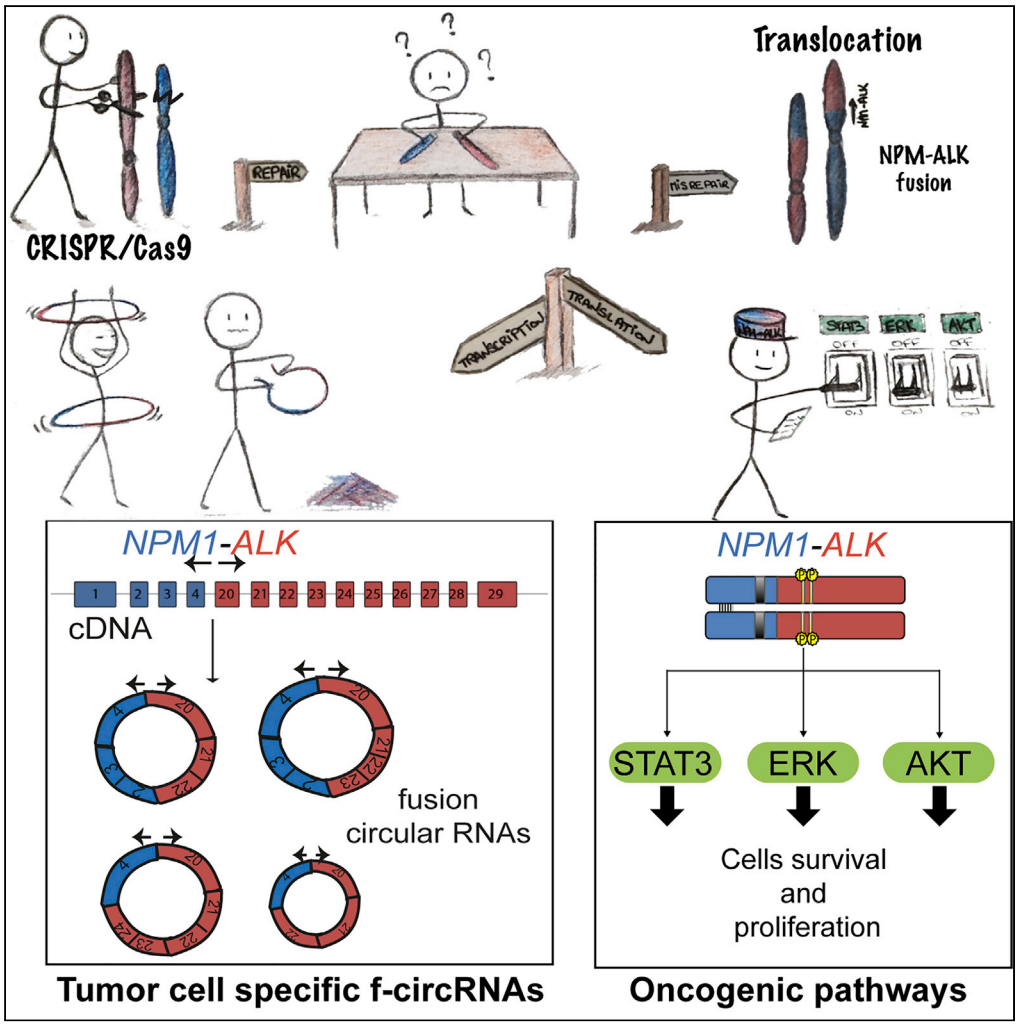

Loelia Babin, Marion Piganeau, Benjamin Renouf, ..., Thomas Mercher, Carine Giovannangeli, Erika C. Brunet

erika.brunet@inserm.fr

HIGHLIGHTS

CRISPR/Cas9 model of ALCL translocation leads to oncogene pathway activation

CRISPR/Cas9 translocations generate *de novo* fusion circular RNAs

Shared fusion circular RNAs are found in CRISPR/Cas9 models and ALCL tumor cells

Babin et al., iScience 5, 19–29
July 27, 2018
https://doi.org/10.1016/j.isci.2018.06.007

iScience

CellPress

Article

Chromosomal Translocation Formation Is Sufficient to Produce Fusion Circular RNAs Specific to Patient Tumor Cells

Loelia Babin,[1,2,6] Marion Piganeau,[2,5,6] Benjamin Renouf,[2] Khadija Lamribet,[2] Cecile Thirant,[3] Ludovic Deriano,[4] Thomas Mercher,[3] Carine Giovannangeli,[2] and Erika C. Brunet[1,2,7,*]

SUMMARY

Circular RNAs constitute a unique class of RNAs whose precise functions remain to be elucidated. In particular, cancer-associated chromosomal translocations can give rise to fusion circular RNAs that play a role in leukemia progression. However, how and when fusion circular RNAs are formed and whether they are being selected in cancer cells remains unknown. Here, we used CRISPR/Cas9 to generate physiological translocation models of NPM1-ALK fusion gene. We showed that, in addition to generating fusion proteins and activating specific oncogenic pathways, chromosomal translocation induced by CRISPR/Cas9 led to the formation of *de novo* fusion circular RNAs. Specifically, we could recover different classes of circular RNAs composed of different circularization junctions, mainly back-spliced species. In addition, we identified fusion circular RNAs identical to those found in related patient tumor cells providing evidence that fusion circular RNAs arise early after chromosomal formation and are not just a consequence of the oncogenesis process.

INTRODUCTION

Circular RNAs (circRNAs) were discovered in eukaryotic cells more than 30 years ago (Hsu and Coca-Prados, 1979) but were first classified as splice errors (Cocquerelle et al., 1993). Only recently new reports showing the emerging role of circRNAs in multiple biological functions drew renewed attention to this specific repertoire of non-coding RNAs (Hansen et al., 2013; Jeck et al., 2013). In particular, recent advances in high throughput sequencing showed high abundance and conservation of circRNAs among species. Biogenesis of circRNAs remains unclear, but different mechanisms have been described that are associated with canonical and non-canonical splicing, and with the presence of repeat sequences in the introns surrounding the junction of circularization (Conn et al., 2015; Errichelli et al., 2017; Ivanov et al., 2015; Zhang et al., 2013, 2016). CircRNAs can act as transcription regulators (Li et al., 2015), microRNA sponges (Hansen et al., 2013; Memczak et al., 2013; Chen et al., 2017), or platforms for RNA binding proteins (Ashwal-Fluss et al., 2014). In addition, a small subset of circRNAs is translated (Pamudurti et al., 2017). Recently, circRNAs have been shown to be implicated in cell differentiation (Legnini et al., 2017) and to be associated with human diseases (Chen et al., 2017; Hsiao et al., 2017; Shao and Chen, 2016) and could be used as diagnostic biomarkers (Lu et al., 2017). A study from Pandolfi's laboratory demonstrated that chromosomal translocations lead to the expression of fusion-specific circRNAs in various types of tumor cells (Guarnerio et al., 2016).

Recurrent cancer translocations disrupt tumor suppressors, activate oncogenes, or generate aberrant fusion proteins. Expression of the resulting fusion cDNA has been the main strategy to study translocation-driven oncogenesis. Although this strategy provides valuable insights and understanding regarding the role of several specific translocations, the outcome does not always phenocopy the respective disease and may not accurately recapitulate the multistep process of translocation-driven oncogenesis. For instance, TEL-AML1 knock-in mice remain without evidence of disease, and treatment of these animals with mutagenic compounds mainly induces T cell malignancies without characteristics of B-ALL as observed in humans (Schindler et al., 2009). Particularly, overexpression of fusion cDNA hardly reproduces physiological expression of the fusion gene (dosage effects) and does not take into account other potential oncogenic consequences of translocations including reciprocal fusion gene formation, disruption of endogenous fused genes, or transcriptional and epigenetic changes resulting from repositioning of translocated chromosomes in the nucleus.

[1]Laboratory "Genome Dynamics in the Immune System", Equipe Labellisée Ligue Contre le Cancer, INSERM UMR1163; Université Paris Descartes Sorbonne Paris Cité, Institut Imagine, Paris 75015, France

[2]Museum National d'Histoire Naturelle, INSERM U1154, CNRS UMR7196, Sorbonne Université, Paris 75005, France

[3]INSERM U1170, Equipe Labellisée Ligue Contre le Cancer, Gustave Roussy Institute, Université Paris Diderot, Université Paris-Sud, Villejuif 94800, Francet

[4]Genome Integrity, Immunity and Cancer Unit, Department of Immunology, Department of Genomes and Genetics, Institut Pasteur, Paris 75015, France

[5]Present Address: Haematopoietic Stem Cell Lab, The Francis Crick Institute, London NW1 1AT, UK

[6]These authors contributed equally

[7]Lead Contact

*Correspondence: erika.brunet@inserm.fr

https://doi.org/10.1016/j.isci.2018.06.007

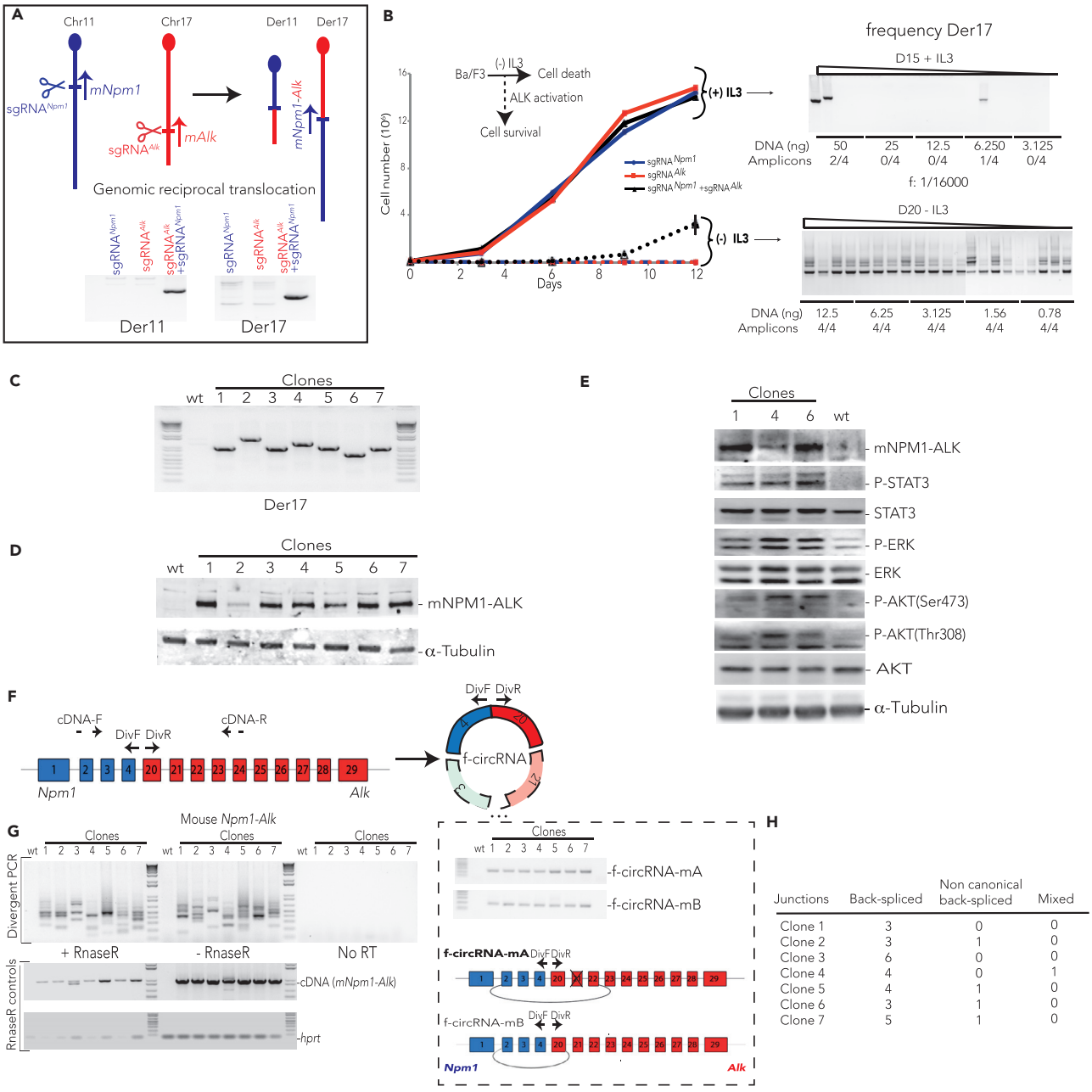

Figure 1. *NPM1-ALK* Translocation Induces Ba/F3 Cells Transformation and Leads to f-circRNA Formation

(A) In mouse cells, *Npm1* and *Alk* genes are located on chromosomes 11 and 17, respectively. To induce t(11; 17) translocation, CRISPR/Cas9 system is used to create specific *Npm1* (using sgRNA^{Npm1}) and *Alk* (using sgRNA^{Alk}) DSBs. The derivative chromosome 17 (Der17) will lead to *Npm1-Alk* fusion gene expression. Both derivative chromosomes, Der11 and Der17, are recovered only when *Npm1* and *Alk* DSBs are concomitantly induced (detected by nested PCR).

(B) Proliferation curve of CRISPR/Cas9-treated cells after IL-3 removal. Left panel: cytokine-independent growth was observed only from cells originating from the pool treated with sgRNA^{Npm1} and sgRNA^{Alk} (mean of three experiments ± SD). Right panels: estimate of translocation frequency using PCR on serial dilutions of genomic DNA from Ba/F3 cells. The number of times the PCR was positive for each dilution is indicated (amplicons) (from four independent experiments). At day 15 after transfection (upper panel), translocation junction from cells cultured with IL-3 was detected in two wells of 50 ng DNA, reflecting a frequency around 6.25×10^{-5}. Instead, serial dilutions of DNA from cells growing in the absence of IL-3 (lower panel) showed PCR amplicons for all DNA dilutions (the gel showing all the dilutions is the result of the association of two consecutive gel lines).

(C) PCR amplification of Der17 from seven clones growing without IL-3.

(D) Western Blot analysis of NPM1-ALK expression. Each of the seven clones expressed NPM1-ALK fusion protein.

(E) Western Blot detection of STAT3, AKT, and ERK1/2 phosphorylation for clones 1, 4, and 6. STAT3, AKT, and ERK1/2 activation was detected in all clones.

Figure 1. *Continued*

(F) PCR strategy to detect fusion circular RNAs (f-circRNAs) using divergent primers (DivF and R). Convergent primers (cDNA-F and R) are used to detect linear fusion mRNA (*Npm1* exons in blue and *Alk* exons in red).

(G) PCR-amplified products obtained using divergent primers to detect f-circRNAs corresponding to *Npm1-Alk* gene in Ba/F3 cells (wild-type cells and seven translocated clones). Representative gel from three independent experiments. Schemes of f-circRNA-mA and f-circRNA-mB (right panel) detected in the clones. f-circRNA-mA and f-circRNA-mB were amplified with specific primers.

(H) Number of circular junctions sequenced for each different type of f-circRNA (back-spliced, non-canonical back-spliced, and mixed). Sequencing was done from three independent experiments.

See also Figure S1 and Table S1.

The consistent advances in programmable nuclease technology, including ZFNs (zinc-finger nucleases), TALENs (transcription activator-like effector nucleases), and CRISPR/Cas9 RNA-guided nucleases, facilitates easier and more precise genome editing. Particularly, we and others have shown that introduction of DNA double-strand breaks (DSBs) at patient translocation breakpoints enables specific oncogenic translocation formation (Brunet et al., 2009; Piganeau et al., 2013; Choi and Meyerson, 2014; Ghezraoui et al., 2014; Torres et al., 2014).

In this study, we used CRISPR/Cas9 technology to induce specific chromosomal translocations. We managed to assess immediate cellular consequences, including newly expressed fusion circular RNAs (f-circRNAs). Focusing on *NPM1-ALK* fusion found in anaplastic large cell lymphoma (ALCL) (Morris et al., 1994), we confirmed that CRISPR-induced *NPM1-ALK* translocation was not only sufficient to trigger murine Ba/F3 pro-B cell line transformation but also induced the activation of STAT3, MEK/ERK, and AKT pathways, which are upregulated in ALCL tumors. We demonstrated that newly formed translocations lead to direct expression of specific f-circRNAs transcribed from the *NPM1-ALK* breakpoint junction. Sequencing of f-circRNAs reveals different types of circularization junctions. Strikingly, f-circRNAs found in tumor cell lines of patients with ALCL were also identified in our different translocation models. Thus, our study provides strong evidences that different f-circRNAs, including specific f-circRNAs, found in patient tumor cells are expressed directly after *de novo* translocation induction. These results further support the use of CRISPR/Cas9 to induce *in situ* translocations to reach more relevant cancer models including expression of *de novo* f-circRNAs.

RESULTS

CRISPR/Cas9-Induced NPM1-ALK Fusion Leads to STAT3, AKT, and ERK Pathway Activation in Mouse Cells

NPM1-ALK is an oncogenic fusion protein that is capable of transforming multiple rodent cell lines (Bai et al., 1998; Fujimoto et al., 1996). Particularly, human NPM1-ALK overexpression has been shown to confer interleukin (IL)-3-independent survival and proliferation of Ba/F3 murine pro-B lymphocytes (Bai et al., 1998). In the mouse genome, *Npm1* and *Alk* genes are located on chromosomes 11 and 17, respectively. NPM1-ALK is expressed from the derivative chromosome 17 (Der17) (Figure 1A). We designed single guide (sgRNAs) targeting murine *Npm1* intron 4 and *Alk* intron 19 to induce concomitant DSBs at loci found as breakpoints in human ALCL. Transient co-expression of Cas9 with $sgRNA^{Npm1}$ and $sgRNA^{Alk}$ led to the formation of the two derivative chromosomes (Der11 and Der17). In contrast, a single break on *Npm1* or *Alk* was not sufficient to induce translocation (Figure 1A). The frequency of translocation at day 5 after transfection was $\geq 2.5 \times 10^{-4}$ (Figure S1A) (as calculated in [Renouf et al., 2014]). However, the translocation frequency of cells growing in the presence of IL-3 dropped to 6.25×10^{-5} at day 15 after transfection, indicating that *Npm1-Alk* does not provide a growth advantage in these conditions (Figure 1B). To investigate the ability of CRISPR/Cas9-induced *Npm1-Alk* translocation to transform Ba/F3 cells, we removed IL-3 from the medium of transfected cells. IL-3 withdrawal led to major growth arrest and cell death when cells were treated with a single sgRNA. In contrast, after 6 days without IL-3, we observed proliferation of cellular clones from the pool treated with both $sgRNA^{Npm1}$ and $sgRNA^{Alk}$. After 20 days, we were able to recover multiple translocation junctions. We assessed translocation frequency in proliferating cells without IL-3 and detected Der17 junctions starting from as little as 0.8 ng of DNA, suggesting that most cells carried translocation (Figure 1B). Thus, we confirmed that CRISPR/Cas9-induced mouse *Npm1-Alk* translocation leads to the transformation of Ba/F3 cells as recently shown (van de Krogt et al., 2017). In addition, to validate that IL-3-independent proliferation was driven by constitutive activation of NPM1-ALK, we treated the cells with crizotinib, an ALK phosphorylation inhibitor. We found that crizotinib led to complete proliferation arrest of selected cells in the absence of IL-3, indicative of active NPM1-ALK fusion protein in the whole population (Figure S1B).

We then isolated seven random Ba/F3 clones from cells growing without IL-3. We could detect Der17 in all of them, further confirming the observation that translocations had occurred in IL-3-independent cells (Figure 1C). Importantly, NPM1-ALK fusion protein was expressed in all the clones (Figure 1D). Insertions and deletions were detected at the translocation junctions but restricted to the intronic region between *Npm1* and *Alk* genes (Figure S1C). We further analyzed three clones (clones 1, 4, and 6). Each of them showed clear co-localization between one *Npm1* and one *Alk* signal as observed by fluorescence *in situ* hybridization (FISH) (Figure S1D). *In vitro* and *in vivo* studies have shown that NPM1-ALK kinase promotes cell growth, cell cycle progression, and survival through transphosphorylation of cytosolic targets, including effector proteins of STAT3, MEK/ERK, and AKT pathways (Marzec et al., 2007a, 2007b; Zamo et al., 2002; Zhang et al., 2002). We therefore wondered if *de novo* mouse t(11; 17) translocation induced by CRISPR activates the same signaling cascades. We showed that STAT3 was expressed both in surviving clones and wild-type Ba/F3 cells. However, phosphorylated STAT3 was exclusively detected in the three NPM1-ALK-positive clones, indicating that newly formed NPM1-ALK activates the STAT3 pathway. Similarly, the phosphorylation of ERK1/2 protein was substantially enhanced in the three translocated clones compared with wild-type cells and we could observe greater phosphorylation of specific phospho-sites of AKT (Ser473 and Thr308) (Figure 1E). Our results clearly demonstrate that CRISPR-induced *Npm1-Alk* translocation is sufficient to trigger transformation of murine Ba/F3 pro-B cell line through the activation of ALCL-specific oncogenic pathways.

De Novo Npm1-Alk Translocation Leads to Expression of Circular RNAs Specific to Breakpoint Junctions (f-circRNAs) in Mouse Cells

Recently, f-circRNAs expressed from translocation junctions have been identified in various tumor cells associated with *PML-RARα, MLL-AF9, EWSR1-FLI1,* or *EML4-ALK1* translocation (Guarnerio et al., 2016). This work demonstrated that the presence of *MLL-AF9*-specific f-circRNAs contributes to cell survival upon therapy and plays an active role in leukemia progression *in vivo*. Thus, we wondered if *de novo* translocation formation leads to the expression of f-circRNAs specific to the breakpoint junction. We amplified f-circRNAs using outward-facing PCR primers around the *Npm1-Alk* translocation junction, after RnaseR treatment of our samples to decrease the quantity of linear RNAs as previously described (Guarnerio et al., 2016) (Figures 1F and 1G). Importantly, no f-circRNAs could be amplified in wild-type Ba/F3 cells. We investigated the formation of f-circRNAs in the Ba/F3 clones growing in the absence of IL-3, positive for *NPM1-ALK* translocation. Several PCR amplicons could be detected in each of the seven clones, indicating that f-circRNAs are specific to *de novo* translocation (Figures 1G and 1H). To validate that our amplicons result from f-circRNA formation in cells and are not amplified from the linear *Npm1-Alk* counterpart, we transcribed *in vitro* the *NPM1-ALK* cDNA from human ALCL cells (homology between mouse and human of *NPM1-ALK* exons is >80%), and in parallel, an identified f-circRNA containing six exons as positive control (f-circRNA-hF described in the following section) (Figure S1E). After RT-PCR and PCR amplification using similar conditions as for f-circRNA amplification (in the presence of 1 μg RNA from wild-type cells and with RnaseR treatment), we could detect some PCR amplicons using divergent primers and starting from as less as 1 ng of the linear *NPM1-ALK in vitro* transcript. Sequencing revealed that these unspecific amplicons (18 sequences) corresponded exclusively to sequences containing short direct repeats located at an intra-exonic junction between *NPM1* and *ALK* (Table S1). These unspecific products have been considered as PCR artifacts and have subsequently been excluded from our datasets. More precisely, we excluded every sequence with at least 1 bp found in common at the breakpoint between *NPM1* and *ALK* intra-exonic sequences.

We sequenced four to seven random PCR products from *Npm1-Alk* clones 1 to 7. After excluding PCR artifacts, we defined three different groups of f-circRNAs: (1) back-spliced f-circRNAs reflecting proper back-spliced events (circularized from two canonical splice sites), (2) non-canonical back-spliced f-circRNAs (circularized within two exons that probably arise from alternative splice sites), and (3) mixed f-circRNAs (circularized from one canonical splice site to a site located within an exon) (Figure 1H and Table S1). Of note, some f-circRNAs showed exon skipping (for example, f-circRNA-mA loses the exon 21, Figure 1G). This phenomenon could be similar to circRNAs described by Zhao's team and was called alternative splicing events (Gao et al., 2016). We could identify back-spliced f-circRNAs in every clone (three to six for each clone), and importantly, sequencing revealed that some back-spliced f-circRNAs could be found in several clones (Table S1). We could detect f-circRNA-mA (joining exon 2 of *Npm1* to exon 22 of *Alk*) and f-circRNA-mB (joining exon 2 of *Npm1* to exon 20 of *Alk*) in each of our seven clones by using specific PCR amplification (Figure 1G). In conclusion, *Npm1-Alk*-translocated mouse clones expressed different types of f-circRNAs. Two of them are commonly expressed in all clones, indicating a potential selection process of specific f-circRNAs upon transformation of Ba/F3 cells.

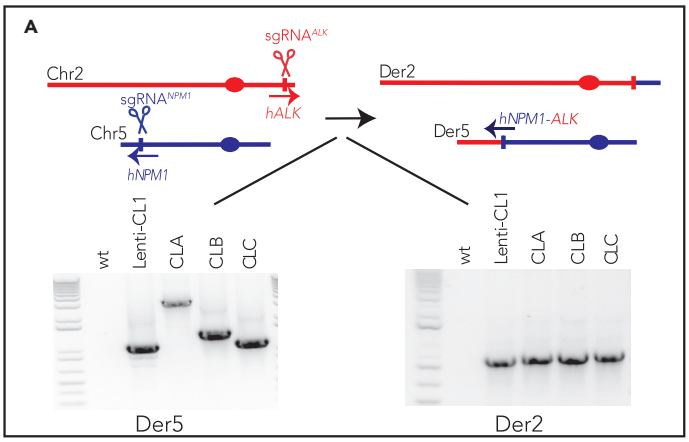

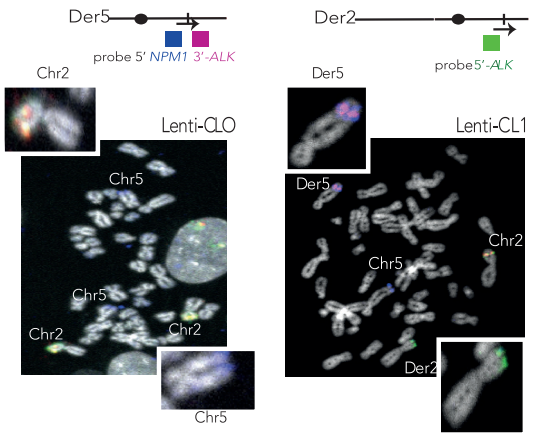

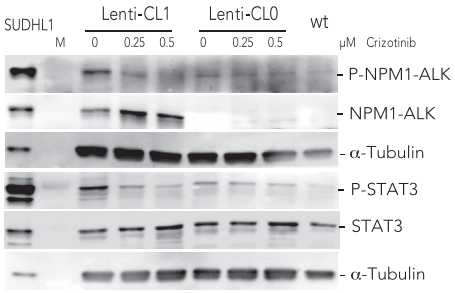

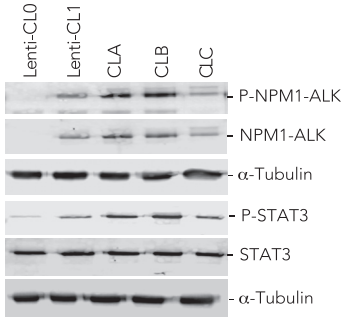

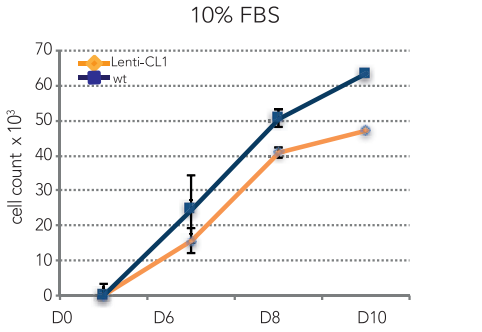

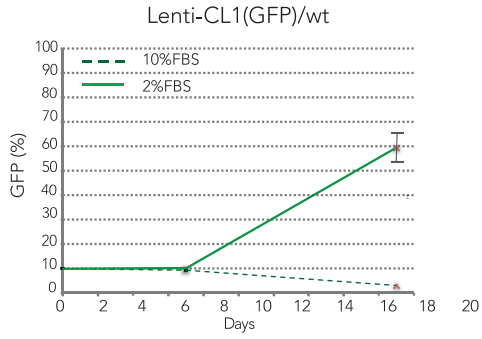

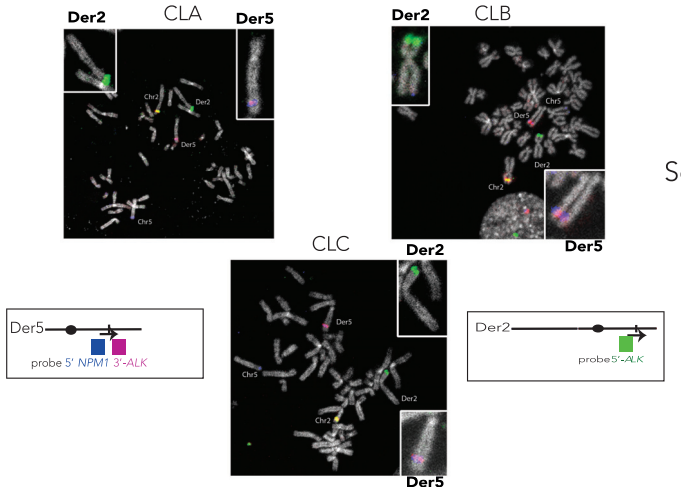

Selection of clones in 2% FBS

Figure 2. NPM1-ALK Activates STAT3 Pathway and Increases Cell Growth in Low-Serum Culture

(A) In human cells, *NPM1* and *ALK* genes are located on chromosomes 5 and 2, respectively. To induce t(2; 5) translocation, CRISPR/Cas9 system is used to induce specific *NPM1* (using $sgRNA^{NPM1}$) and *ALK* (using $sgRNA^{ALK}$) DSBs. The derivative chromosome (Der5) will lead to *NPM1-ALK* fusion gene expression. Der5 and Der2 junctions were detected in the four clones Lenti-CL1 (obtained using a lentivirus vector), CLA, CLB, and CLC isolated from $sgRNA^{NPM1}$- and $sgRNA^{ALK}$-treated cells.

(B) FISH for *NPM1* and *ALK* detection in Lenti-CL0 (control clone) and Lenti-CL1 metaphases. ALK locus is detected with a break-apart probe (green + purple). Blue signal corresponds to the 5′ end *NPM1* locus: Der5 and Der2 formation leads to split purple and green signals. Colocalization of purple and blue signals reveals Der5 formation.

(C) Western blot detection of NPM1-ALK and STAT3 activation in the translocated clones. SUDHL1 is an ALK-positive ALCL cell line. Lenti-CL0 and Lenti-CL1 were also treated with different amounts of crizotinib.

(D) Upper panel: growth curve of wild-type RPE-1 cells and Lenti-CL1 in 10% FBS. Lower panel: competitive proliferation assay between wild-type RPE-1 cells and Lenti-CL1 in the presence of 10% or 2% FBS. Lenti-CL1 stably expressed GFP (mean of three experiments ± SD).

(E) FISH analysis of RPE-1 clones growing in 2% FBS: CLA, CLB, and CLC. A break-apart probe (purple and green) was used for *ALK* and a BAC probe (blue) was used to probe *NPM1*. Der5 and Der2 formation leads to split purple and green signals. Colocalization of purple and blue signals reveals Der5 formation. See also Figure S2.

CRISPR/Cas9-Induced NPM1-ALK Fusion Leads to STAT3 Pathway Activation, Growth Advantage in Low-Serum Medium, and Expression of Specific f-circRNAs in Human Cells

We further decided to confirm the formation of f-circRNAs in a human cell line after *NPM1-ALK* formation. We first induced t(2; 5) (p23; q35) translocation in the human RPE-1 hTERT-immortalized retinal pigment epithelial cell line, which has a near-diploid karyotype, making it relevant to analyze chromosomal rearrangements. We previously set up the CRISPR/Cas9 transfection system to efficiently induce t(2; 5) (p23; q35) in RPE-1 cells using sgRNAs targeting *NPM1* intron 4 and *ALK* intron 19 (Ghezraoui et al., 2014; Renouf et al., 2014). However, in these studies, we failed to efficiently recover translocated clones. Here we adapted a lentiviral strategy (Heckl et al., 2014) to stably integrate the Cas9 nuclease and the two sgRNAs targeting *NPM1* and *ALK* (Figure S2A). After transduction and fluorescence-activated cell sorting (FACS) sorting of transduced cells, we isolated one *NPM1-ALK* positive clone (Lenti-CL1) and one *NPM1-ALK*-negative clone (Lenti-CL0) confirmed by FISH analysis (Figures 2A and 2B). Sequencing of derivative chromosome junctions confirmed the formation of fusion junctions in Lenti-CL1 (Figure S2A). NPM1-ALK fusion protein was stably expressed and active as shown by its auto-phosphorylation (Figure 2C). Importantly, the phosphorylation dropped back to background level upon crizotinib treatment. Similarly, STAT3 showed enhanced phosphorylation in Lenti-CL1 clone compared with negative Lenti-CL0 cells and phosphorylation went back to a basal level with crizotinib treatment, indicating a reliance on NPM1-ALK activity. Of note, RPE-1 cells have high endogenous ERK1/2 and AKT phosphorylation, preventing the assessment of NPM1-ALK-driven phosphorylation for those pathways. Intriguingly, crizotinib treatment had no discernable effect on cell growth or survival of Lenti-CL1 using normal culture conditions (data not shown). Instead, wild-type cells grew faster than Lenti-CL1 cells in 10% of fetal bovine serum (FBS) (Figure 2D), possibly explaining the difficulties we previously faced in isolating translocated cells by traditional cloning method. Thus, as for Ba/F3 cells, we also observed a dramatic decrease in the frequency of translocated cells over time for cells transfected with $sgRNA^{NPM1}$ and $sgRNA^{ALK}$. This phenomenon was independent of the initial frequency of translocation (5×10^{-4} [high] or 1.25×10^{-4} [low] [Figure S2B]). These results prompted us to test the growth of *NPM1-ALK* clone in the presence of low serum concentration (2% FBS). In this condition, Lenti-CL1 (GFP-positive cells) showed then a strong proliferative advantage over wild-type cells (2% FBS) (Figure 2D) and the translocation frequency increased up to 16-fold after 16 days (Figure S2B). These experiments strongly indicate that *NPM1-ALK* translocation led to a marked growth advantage in culture conditions containing lower growth factor concentrations. Thus we envisioned that the recovery of translocated clones would be enhanced by culturing $sgRNA^{NPM1}$- and $sgRNA^{ALK}$-transfected cells in 2% FBS medium. As expected, we easily isolated three additional *NPM1-ALK*-positive clones by simple cloning using low-serum medium (CLA, CLB, and CLC; Figures 2A and S2A). These clones were translocated as shown by FISH (Figure 2E) and expressed an active form of NPM1-ALK, leading to STAT3 phosphorylation (Figure 2C).

We next looked for the formation of f-circRNAs in our different human RPE-1 clones carrying *NPM1-ALK* translocation (Figure 3A). As for mouse cells, no f-circRNA could be amplified from wild-type cells. In contrast, several PCR products were detected and sequenced from all four *NPM1-ALK* clones (Figures 3A and 3B and Table S2). *NPM1-ALK* translocation induced in human cells also led to the expression of the three different types of f-circRNAs. Importantly, four back-spliced f-circRNAs were found common in all clones (Figure 3A and Table S2). Here we also confirmed that our treatment with RnaseR specifically

A

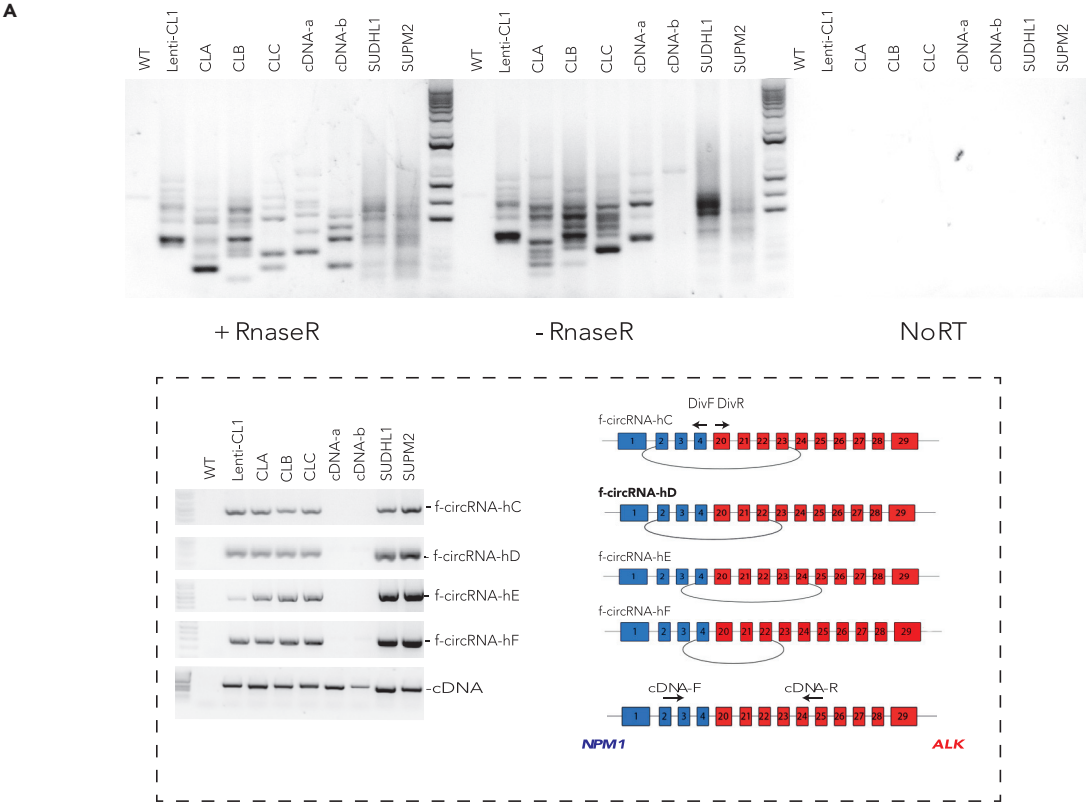

B

Junctions	Back-spliced	Non-canonical back-spliced	Mixed
Lenti-CL1	7	1	1
CLA	6	0	0
CLB	5	1	0
CLC	5	0	0
cDNA-a	0	0	0
cDNA-b	0	1	0
SUDHL1	10	0	4
SUPM2	6	1	1

C

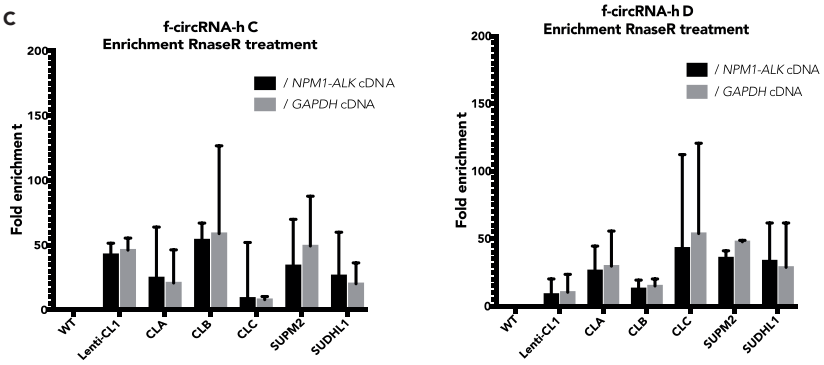

D

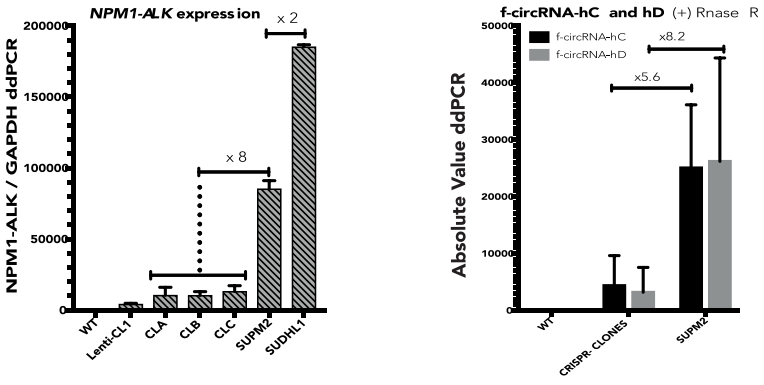

Figure 3. *NPM1-ALK* Induces the Expression of ALCL-Specific f-circRNAs

(A) PCR-amplified products obtained using divergent primers to detect f-circRNAs corresponding to *NPM1-ALK* gene in RPE-1 human cells: from wild-type cells, CRISPR/Cas9-translocated clones, cells overexpressing NPM1-ALK (labeled cDNA-a and cDNA-b), and SUDHL1 and SUPM2 ALCL cells. Representative gel from three independent experiments. Schemes of f-circRNA-hC, f-circRNA-hD, f-circRNA-hE, and f-circRNA-hF (middle panel) shared by Lenti-CL1, CLA, CLB, CLC, SUDHL1, and SUPM2 cells. The PCR product corresponding to f-circRNA-hD (bold) has similar circularization junction as f-circRNA-mA in Ba/F3 cells (Figure 1A). f-circRNA-hC, f-circRNA-hD, f-circRNA-hE, and f-circRNA-hF were also amplified with specific primers. Detection of *NPM1-ALK* fusion gene (cDNA) was done using the convergent primers.

(B) Number of circular junctions sequenced for each type of *NPM1-ALK* f-circRNA in RPE-1 and ALCL cells (back-spliced, non-canonical back-spliced, and mixed). Sequencing was done from three independent experiments.

(C) Fold enrichment for f-circRNA-hC/ f-circRNA-hD after RnaseR treatment normalized by *NPM1-ALK* linear cDNA and *GAPDH* cDNA (mean of three experiments ± SEM).

(D) Left panel: *NPM1-ALK* linear cDNA expression level in CRISPR/Cas9 clones and SUPM2 and SUDHL1 cells. Right panel: f-circRNA-hC or f-circRNA-hD expression level in CRISPR clones compared with SUPM2 cells (average from all the clones) (mean of three experiments ± SEM).

See also Figure S3 and Table S2.

diminished the quantity of linear RNAs compared with the identified f-circRNAs (from 8- to 50-fold as quantified in Figure 3C), decreasing the potential background of PCR due to unspecific amplification from linear cDNA (described in the previous section).

Furthermore, we generated RPE-1 clones stably expressing human *NPM1-ALK* cDNA (named cDNA-a and cDNA-b). *NPM1-ALK* expression was confirmed by PCR amplification of fusion cDNA (Figure 3A). In our conditions of amplification and after excluding PCR artifacts, only one non-canonical back-spliced f-circRNA has been detected in clones expressing *NPM1-ALK* cDNA (Figure 3B and Table S2), in contrast to cells carrying translocated chromosomes, which expressed more f-circRNAs and mostly canonical back-spliced f-circRNAs.

One particular f-circRNA from *MLL-AF9* fusion was extensively studied by Guarnerio et al. (2016) and found as tumor specific. Thus, to further investigate the circRNA repertoire formed after CRISPR-induced translocation, we designed a translocation system for *Mll-Af9* fusion (Drynan et al., 2005). We could reproduce the translocation in a mouse pro-B cell line and obtained three translocated clones for *Mll-Af9* genes as confirmed by PCR amplification of the derivative chromosomes, *Mll-Af9* cDNA amplification, and FISH analysis (Figures S3A and S3B). We could readily detect different types of f-circRNAs, and some back-spliced f-circRNAs were prevalent in all clones, as observed for *NPM1-ALK* model (Figure S3C). For instance, back-spliced f-circRNA-mG and f-circRNA-mH were found in each of the three clones (Figure S3C and Table S3). These preliminary results validate that common f-circRNAs are generated by the formation of endogenous *Mll-Af9* translocation, as observed for the *NPM1-ALK* model. Further validation by RNA-seq in human CRISPR/Cas9 clones would be needed.

In conclusion, the formation of derivative chromosomes using CRISPR/Cas9 technology leads to a specific landscape of f-circRNAs.

De Novo NPM1-ALK Translocation Leads to the Expression of f-circRNAs Specific to Human ALCL Tumor Cells

To gain insight into the relevance of the repertoire of f-circRNAs formed in our clones, we compared them with the ones found in ALCL tumor cells, SUDHL1 and SUPM2 cell lines. As for the RPE-1 clones, we recovered all types of f-circRNAs in the two ALCL cell lines. Notably, the four back-spliced f-circRNAs shared by all *NPM1-ALK* RPE-1 clones induced by CRISPR/Cas9 were also expressed in SUDHL1 and in SUPM2 patient cells: f-circRNA-hC joining exon 2 to exon 23, f-circRNA-hD joining exon 2 to exon 22, f-circRNA-hE joining exon 4 to exon 24, and f-circRNA-hF joining exon 4 to exon 22 (Figure 3A and Table S2). Remarkably, f-circRNA-hD, which circularized the exon 2 of *NPM1* to the exon 22 of *ALK*, was also expressed in all the mouse *Npm1-Alk*-positive clones (corresponding to f-circRNA-mA, Figure 1G). We then estimate the relative expression level of two of the four common f-circRNAs. The level of f-circRNA-hC and f-circRNA-hD in CRISPR/Cas9 clones was found to be 5- to 8-fold lower than in SUPM2 tumor cells. This level directly correlates to the difference of expression of *NPM1-ALK* cDNA between the clones and the tumor cells (of note SUDHL1 tumor cells contain two copies of the translocation, leading to 2-fold higher expression of *NPM1-ALK* compared with SUPM2 cells) (Figure 3D).

Thereby CRISPR/Cas9 approach to induce translocation leads to modifications of the non-coding RNA repertoire by expressing tumor-related f-circRNAs.

DISCUSSION

Here, we successfully used CRISPR/Cas9 nucleases to induce *de novo* chromosomal translocations leading to *NPM1-ALK* fusion oncogene expression in mouse and human cell lines. We confirmed that endogenous mouse NPM1-ALK expression is sufficient to confer cytokine-independent growth of mouse cells as recently shown by the group of Wlodarska (van de Krogt et al., 2017). Furthermore, we demonstrated that the cell survival depended on NPM1-ALK activation and was inhibited by crizotinib treatment. CRISPR/Cas9-mediated rearranged mouse and human cell lines displayed STAT3 (for our human cells), AKT, and ERK1/2 phosphorylation depending on NPM1-ALK kinase expression and activity. Activation of these three proteins was found essential for cell transformation and tumor maintenance in cancer cells (Marzec et al., 2007b; Zamo et al., 2002; Zhang et al., 2002). In addition, low concentrations of growth factors favored proliferation of translocated clones over wild-type cells. This observation is consistent with the fact that NPM1-ALK fusion protein expressed at physiological levels can substitute cytokine stimulation. In conditions in which wild-type cells grow easily (10% serum), translocated cells are probably diluted before acquiring any advantage phenotype.

Our results demonstrated that *de novo* translocation formation promptly leads to the expression of *de novo* circRNAs specific to the fusion breakpoint. Interestingly, f-circRNAs found in cancer-associated chromosomal translocation have already been shown to participate in cellular transformation (Guarnerio et al., 2016). In this study, expression of a specific f-circRNA in hematopoietic stem cells (containing the MLL-AF9 fusion) led to a proliferative advantage and favored the progression of leukemia *in vivo*, demonstrating a physiological role for f-circRNAs. To gain further insight into f-circRNA formation, we generated CRISPR-mediated translocations. We observed the expression of several f-circRNAs upon translocation formation encompassing from two to nine exons (with a length up to 980 bp). The fact that several different f-circRNAs were expressed from the same fusion gene is quite surprising, and whether or not they all have a physiological role remains to be determined. The presence of specific exons may also have a particular biological relevance. Remarkably, we identified specific f-circRNAs expressed in translocated clones perfectly matching those found in tumor-related cells. We also recovered one specific f-circRNA (f-circRNA-mA and f-circRNA-hD) in our mouse and human *NPM1-ALK*-positive clones, respectively, that was also expressed in two ALCL cell lines, supporting the idea that circRNAs are well conserved between human and mouse cells (Legnini et al., 2017; Rybak-Wolf et al., 2015).

Several types of f-circRNAs were identified in this study. Importantly, CRISPR/Cas9 *NPM1-ALK*-translocated clones showed a different f-circRNA repertoire compared with clones that expressed ectopically *NPM1-ALK* cDNA. Several back-spliced species were expressed in CRISPR/Cas9 clones. This class of f-circRNAs properly joins a 5′ splice site with a 3′ splice site of an upstream intron. These events are thought to arise from the annealing of inverted repeat sequences inside flanking exons, enhancing the juxtaposition of the splice sites leading to back-splicing (Jeck et al., 2013). The f-circRNAs that were found common to several clones and tumor cells (but not in cells ectopically expressing *NPM1-ALK* cDNA) were exclusively canonical back-spliced f-circRNAs, in agreement with their identification in earlier RNA-seq studies.

Surprisingly, *in vitro* transcription revealed that unspecific PCR amplicons can be generated when amplifying linear cDNA using classical divergent PCR designed for circRNAs. All these events exhibit short direct repeats for at least 1 bp located at the circularized junction between *NPM1* and *ALK*. They are probably produced after PCR template switching, although we can wonder if 1 bp is enough to lead to efficient polymerase template switch. Efficient treatment with RnaseR is then essential for decreasing false-positives from these types of experiments. Instead, we kept mixed events where no repeat could be found, indicating that these types of PCR products were not found as amplified from linear cDNA. The relevance of these forms of f-circRNA (which probably reflect the presence of non-canonical back-spliced sites) remains to be elucidated in further RNA sequencing (RNA-seq) studies. In conclusion, the CRISPR/Cas9 strategy to induce chromosomal translocation provides experimental settings where *de novo* f-circRNAs are formed: this method will certainly help to precisely dissect the biogenesis and the functional roles of circRNAs since *de novo* circRNAs can be easily tracked.

To conclude, our study provides evidence that f-circRNAs found in tumor cells are produced directly from newly rearranged chromosomes. Therefore, precise genome rearrangements obtained with CRIPSR/Cas9 provide faithful models phenocopying chromosomal translocation-associated diseases including activation of oncogenic pathways and also expression of tumor-specific f-circRNAs by bypassing limitations of models

expressing the fusion gene ectopically. Identification of specific f-circRNAs could provide new diagnostic markers related to cancer aggressiveness and might become therapeutic targets in the near future.

METHODS

All methods can be found in the accompanying Transparent Methods supplemental file.

DATA AND SOFTWARE AVAILABILITY

Original imaging data have been deposited to Mendeley Data and are available at https://doi.org/10.17632/22mbdtz59s.1 (https://doi.org/10.17632/22mbdtz59s.1).

SUPPLEMENTAL INFORMATION

Supplemental Information includes Transparent Methods, three figures, and four tables and can be found with this article online at https://doi.org/10.1016/j.isci.2018.06.007.

ACKNOWLEDGMENTS

We are very grateful to Dr. S. Kabir for commenting on the manuscript, to Dr. J-P de Villartay/P. Revy lab and to Dr. A. De Cian for scientific feedback, to Dr. F. Megetto for providing Ba/F3 cells, and to Dr. C. Lescale and J. Bianchi for providing pro-B cell lines. This research work is supported by a joint grant (E.B., T.M., and L.D.) from the Institut National du Cancer and the Cancéropôle IdF (2016-1-PLBIO-07-INSERM11-1). E.B. research was supported by ANR-12-JSV6-0005. E.B.'s group and T.M.'s team belong to two "La ligue contre le Cancer" teams. M.P. was supported by fellowships from Le Cancéropole IdF and La Ligue Contre le Cancer, and C.T., by a fellowship from la Fondation de France. L.D.'s research is supported by the Institut Pasteur as well as by the European Research Council under the ERC starting grant agreement # 310917, and T.M.'s research, by SIRIC SOCRATE and an Emergence grant from the Canceropole IdF.

AUTHOR CONTRIBUTIONS

E.C.B conceived the initial study. E.C.B, L.B., and M.P. designed research experiments with the help of L.D., T.M., and C.G. M.P. and L.B. performed most of the experiments, B.R. designed and tested the CRISPR/Cas9 system for NPM1-ALK, and K.L. provided technical support for FISH and protein analysis and for f-circRNA detection. C.T. established the lentiviral transduction and FACS sorting in RPE-1 cells. E.B., L.B., and M.P. wrote the manuscript with valuable feedback from all the authors.

DECLARATION OF INTERESTS

None declared.

Received: December 8, 2017
Revised: May 5, 2018
Accepted: June 14, 2018
Published: July 27, 2018

REFERENCES

Ashwal-Fluss, R., Meyer, M., Pamudurti, N.R., Ivanov, A., Bartok, O., Hanan, M., Evantal, N., Memczak, S., Rajewsky, N., and Kadener, S. (2014). circRNA biogenesis competes with pre-mRNA splicing. Mol. Cell *56*, 55–66.

Bai, R.Y., Dieter, P., Peschel, C., Morris, S.W., and Duyster, J. (1998). Nucleophosmin-anaplastic lymphoma kinase of large-cell anaplastic lymphoma is a constitutively active tyrosine kinase that utilizes phospholipase C-gamma to mediate its mitogenicity. Mol. Cell. Biol. *18*, 6951–6961.

Brunet, E., Simsek, D., Tomishima, M., DeKelver, R., Choi, V.M., Gregory, P., Urnov, F., Weinstock, D.M., and Jasin, M. (2009). Chromosomal translocations induced at specified loci in human stem cells. Proc. Natl. Acad. Sci. USA *106*, 10620–10625.

Chen, L., Zhang, S., Wu, J., Cui, J., Zhong, L., Zeng, L., and Ge, S. (2017). circRNA_100290 plays a role in oral cancer by functioning as a sponge of the miR-29 family. Oncogene *36*, 4551–4561.

Choi, P.S., and Meyerson, M. (2014). Targeted genomic rearrangements using CRISPR/Cas technology. Nat. Commun. *5*, 3728.

Cocquerelle, C., Mascrez, B., Hetuin, D., and Bailleul, B. (1993). Mis-splicing yields circular RNA molecules. FASEB J. *7*, 155–160.

Conn, S.J., Pillman, K.A., Toubia, J., Conn, V.M., Salmanidis, M., Phillips, C.A., Roslan, S., Schreiber, A.W., Gregory, P.A., and Goodall, G.J. (2015). The RNA binding protein quaking regulates formation of circRNAs. Cell *160*, 1125–1134.

Drynan, L.F., Pannell, R., Forster, A., Chan, N.M., Cano, F., Daser, A., and Rabbitts, T.H. (2005). Mll fusions generated by Cre-loxP-mediated de novo translocations can induce lineage reassignment in tumorigenesis. EMBO J. *24*, 3136–3146.

Errichelli, L., Dini Modigliani, S., Laneve, P., Colantoni, A., Legnini, I., Capauto, D., Rosa, A., De Santis, R., Scarfo, R., Peruzzi, G., et al. (2017). FUS affects circular RNA expression in murine embryonic stem cell-derived motor neurons. Nat. Commun. *8*, 14741.

Fujimoto, J., Shiota, M., Iwahara, T., Seki, N., Satoh, H., Mori, S., and Yamamoto, T. (1996). Characterization of the transforming activity of p80, a hyperphosphorylated protein in a Ki-1 lymphoma cell line with chromosomal translocation t(2;5). Proc. Natl. Acad. Sci. USA *93*, 4181–4186.

Gao, Y., Wang, J., Zheng, Y., Zhang, J., Chen, S., and Zhao, F. (2016). Comprehensive identification of internal structure and alternative splicing events in circular RNAs. Nat. Commun. *7*, 12060.

Ghezraoui, H., Piganeau, M., Renouf, B., Renaud, J.B., Sallmyr, A., Ruis, B., Oh, S., Tomkinson, A.E., Hendrickson, E.A., Giovannangeli, C., et al. (2014). Chromosomal translocations in human cells are generated by canonical nonhomologous end-joining. Mol. Cell *55*, 829–842.

Guarnerio, J., Bezzi, M., Jeong, J.C., Paffenholz, S.V., Berry, K., Naldini, M.M., Lo-Coco, F., Tay, Y., Beck, A.H., and Pandolfi, P.P. (2016). Oncogenic role of fusion-circRNAs derived from cancer-associated chromosomal translocations. Cell *165*, 289–302.

Hansen, T.B., Jensen, T.I., Clausen, B.H., Bramsen, J.B., Finsen, B., Damgaard, C.K., and Kjems, J. (2013). Natural RNA circles function as efficient microRNA sponges. Nature *495*, 384–388.

Heckl, D., Kowalczyk, M.S., Yudovich, D., Belizaire, R., Puram, R.V., McConkey, M.E., Thielke, A., Aster, J.C., Regev, A., and Ebert, B.L. (2014). Generation of mouse models of myeloid malignancy with combinatorial genetic lesions using CRISPR-Cas9 genome editing. Nat. Biotechnol. *32*, 941–946.

Hsiao, K.Y., Lin, Y.C., Gupta, S.K., Chang, N., Yen, L., Sun, H.S., and Tsai, S.J. (2017). Noncoding effects of circular RNA CCDC66 promote colon cancer growth and metastasis. Cancer Res. *77*, 2339–2350.

Hsu, M.T., and Coca-Prados, M. (1979). Electron microscopic evidence for the circular form of RNA in the cytoplasm of eukaryotic cells. Nature *280*, 339–340.

Ivanov, A., Memczak, S., Wyler, E., Torti, F., Porath, H.T., Orejuela, M.R., Piechotta, M., Levanon, E.Y., Landthaler, M., Dieterich, C., et al. (2015). Analysis of intron sequences reveals hallmarks of circular RNA biogenesis in animals. Cell Rep. *10*, 170–177.

Jeck, W.R., Sorrentino, J.A., Wang, K., Slevin, M.K., Burd, C.E., Liu, J., Marzluff, W.F., and Sharpless, N.E. (2013). Circular RNAs are abundant, conserved, and associated with ALU repeats. RNA *19*, 141–157.

Legnini, I., Di Timoteo, G., Rossi, F., Morlando, M., Briganti, F., Sthandier, O., Fatica, A., Santini, T., Andronache, A., Wade, M., et al. (2017). Circ-ZNF609 is a circular RNA that can be translated and functions in myogenesis. Mol. Cell *66*, 22–37 e29.

Li, F., Zhang, L., Li, W., Deng, J., Zheng, J., An, M., Lu, J., and Zhou, Y. (2015). Circular RNA ITCH has inhibitory effect on ESCC by suppressing the Wnt/beta-catenin pathway. Oncotarget *6*, 6001–6013.

Lu, L., Sun, J., Shi, P., Kong, W., Xu, K., He, B., Zhang, S., and Wang, J. (2017). Identification of circular RNAs as a promising new class of diagnostic biomarkers for human breast cancer. Oncotarget *8*, 44096–44107.

Marzec, M., Kasprzycka, M., Liu, X., El-Salem, M., Halasa, K., Raghunath, P.N., Bucki, R., Wlodarski, P., and Wasik, M.A. (2007a). Oncogenic tyrosine kinase NPM/ALK induces activation of the rapamycin-sensitive mTOR signaling pathway. Oncogene *26*, 5606–5614.

Marzec, M., Kasprzycka, M., Liu, X., Raghunath, P.N., Wlodarski, P., and Wasik, M.A. (2007b). Oncogenic tyrosine kinase NPM/ALK induces activation of the MEK/ERK signaling pathway independently of c-Raf. Oncogene *26*, 813–821.

Memczak, S., Jens, M., Elefsinioti, A., Torti, F., Krueger, J., Rybak, A., Maier, L., Mackowiak, S.D., Gregersen, L.H., Munschauer, M., et al. (2013). Circular RNAs are a large class of animal RNAs with regulatory potency. Nature *495*, 333–338.

Morris, S.W., Kirstein, M.N., Valentine, M.B., Dittmer, K.G., Shapiro, D.N., Saltman, D.L., and Look, A.T. (1994). Fusion of a kinase gene, ALK, to a nucleolar protein gene, NPM, in non-Hodgkin's lymphoma. Science *263*, 1281–1284.

Pamudurti, N.R., Bartok, O., Jens, M., Ashwal-Fluss, R., Stottmeister, C., Ruhe, L., Hanan, M., Wyler, E., Perez-Hernandez, D., Ramberger, E., et al. (2017). Translation of CircRNAs. Mol. Cell *66*, 9–21 e27.

Piganeau, M., Ghezraoui, H., De Cian, A., Guittat, L., Tomishima, M., Perrouault, L., Rene, O., Katibah, G.E., Zhang, L., Holmes, M.C., et al. (2013). Cancer translocations in human cells induced by zinc finger and TALE nucleases. Genome Res. *23*, 1182–1193.

Renouf, B., Piganeau, M., Ghezraoui, H., Jasin, M., and Brunet, E. (2014). Creating cancer translocations in human cells using Cas9 DSBs and nCas9 paired nicks. Methods Enzymol. *546*, 251–271.

Rybak-Wolf, A., Stottmeister, C., Glazar, P., Jens, M., Pino, N., Giusti, S., Hanan, M., Behm, M., Bartok, O., Ashwal-Fluss, R., et al. (2015). Circular RNAs in the mammalian brain are highly abundant, conserved, and dynamically expressed. Mol. Cell *58*, 870–885.

Schindler, J.W., Van Buren, D., Foudi, A., Krejci, O., Qin, J., Orkin, S.H., and Hock, H. (2009). TEL-AML1 corrupts hematopoietic stem cells to persist in the bone marrow and initiate leukemia. Cell Stem Cell *5*, 43–53.

Shao, Y., and Chen, Y. (2016). Roles of circular RNAs in neurologic disease. Front. Mol. Neurosci. *9*, 25.

Torres, R., Martin, M.C., Garcia, A., Cigudosa, J.C., Ramirez, J.C., and Rodriguez-Perales, S. (2014). Engineering human tumour-associated chromosomal translocations with the RNA-guided CRISPR-Cas9 system. Nat. Commun. *5*, 3964.

van de Krogt, J.A., Vanden Bempt, M., Finalet Ferreiro, J., Mentens, N., Jacobs, K., Pluys, U., Doms, K., Geerdens, E., Uyttebroeck, A., Pierre, P., et al. (2017). ALK-positive anaplastic large cell lymphoma with the variant RNF213-, ATIC- and TPM3-ALK fusions is characterized by copy number gain of the rearranged ALK gene. Haematologica *102*, 1605–1616.

Zamo, A., Chiarle, R., Piva, R., Howes, J., Fan, Y., Chilosi, M., Levy, D.E., and Inghirami, G. (2002). Anaplastic lymphoma kinase (ALK) activates Stat3 and protects hematopoietic cells from cell death. Oncogene *21*, 1038–1047.

Zhang, Q., Raghunath, P.N., Xue, L., Majewski, M., Carpentieri, D.F., Odum, N., Morris, S., Skorski, T., and Wasik, M.A. (2002). Multilevel dysregulation of STAT3 activation in anaplastic lymphoma kinase-positive T/null-cell lymphoma. J. Immunol. *168*, 466–474.

Zhang, X.O., Dong, R., Zhang, Y., Zhang, J.L., Luo, Z., Zhang, J., Chen, L.L., and Yang, L. (2016). Diverse alternative back-splicing and alternative splicing landscape of circular RNAs. Genome Res. *26*, 1277–1287.

Zhang, Y., Zhang, X.O., Chen, T., Xiang, J.F., Yin, Q.F., Xing, Y.H., Zhu, S., Yang, L., and Chen, L.L. (2013). Circular intronic long noncoding RNAs. Mol. Cell *51*, 792–806.

ISCI, Volume *5*

Supplemental Information

Chromosomal Translocation Formation Is Sufficient to Produce Fusion Circular RNAs Specific to Patient Tumor Cells

Loelia Babin, Marion Piganeau, Benjamin Renouf, Khadija Lamribet, Cecile Thirant, Ludovic Deriano, Thomas Mercher, Carine Giovannangeli, and Erika C. Brunet

SUPPLEMENTAL INFORMATION

SUPPLEMENTARY FIGURES

Supplementary Figure 1 (Related to Figure 1)

Characterization of *Npm1-Alk* translocation induced in mouse cells and *in vitro* study of circRNAs amplification.

(A) Estimate of translocation frequency (f) of Der17 formation from Ba/F3 cells, 5 days after transfection, using PCR on serial dilutions of genomic DNA. The number of times the PCR was positive (from 4 experiments) for each dilution is also indicated (Amplicons). (B) Crizotinib treatment of IL-3 independent cells. 100 nM crizotinib treatment prevents growth of IL-3-independent cells with *Npm1-Alk* translocation selected in Figure 1-B (mean of 2 experiments +/-SD).

(C) Sequences of *Npm1-Alk* breakpoint junctions from Ba/F3 isolated clones. Clones 1, 3, 5, 6 and 7 harbor deletions (Δ), and clones 2 and 4 have insertions (+). All indels are restricted to intronic regions.

(D) FISH analysis of Ba/F3 *Npm1-Alk* clones. A red probe labeled the 5' end of the *Npm1* gene and a green probe labeled the 3' end of *Alk* gene. Colocalization of red and green revealed Der17 formation. It is worth noting that Ba/F3 cells are polypoid cells with in an average of 72 (+/- 2.5) chromosomes. They have 5 signals for *Npm1* locus and 4 signals for *Alk* locus.

(E) Schemes for *in vitro* transcription of linear and circular *NPM1-ALK* using the T7-promoter containing primers. After RnaseR treatment and retro-transcription, divergent PCR primers are used to detect circRNAs. Artefact amplicons from the linear *NPM1-ALK* cDNA are visibly detected. In contrast, f-circRNA-hF is properly amplified. As control for RnaseR digestion, we used convergent PCR primers to amplify *hNPM1-ALK* cDNA and *GAPDH*. Scheme of one PCR artefact (using divergent primers) obtained from the linear *NPM1-ALK* cDNA after sequencing (*direct repeats, in this example the repeat is "CCAACG") (see sequences on Table S1).

Supplementary Figure 2 (Related to Figure 2)

Characterization of *NPM1-ALK* translocation induced in human cells

(A) sgRNAs targeting *NPM1* and *ALK* genes were cloned in a lentiviral vector expressing a Cas9-2A-GFP (vector sgRNAs-Cas9-2A-GFP). Sequences of Der5 and Der2 breakpoint junctions from Lenti-CL1, CLA, CLB and CLC RPE-1 clones.

(B) Estimate of translocation frequency (f) using PCR on serial dilutions of genomic DNA (in duplicates) from RPE-1 cells at day 3 (D3) and day 16 (D16) after transfection for independent experiments (starting from a pool of cells with low and high frequency). Cells were either kept in 10% or 2% of FBS.

Supplementary Figure 3 (Related to Figure 3)

Characterization of *MLL-AF9* translocation induced in mouse cells

(A) Schematic representation of the CRISPR/Cas9-induced *Mll-Af9* translocation in mouse cells. PCR amplification shows Der4 and Der9 formation and *Mll-Af9* cDNA is detected in all 3 clones (we were unable to find a specific antibody for mouse MLL or AF9).

(B) FISH analysis of *MLll-Af9* positive clones in mouse B-cell lines. A green probe labelled the 5'end of *Mll* and a red probe the 3' end of *Af9*. Red and green colocalization signal shows the formation of Der9.

(C) PCR-amplified products obtained using divergent primers to detect f-circRNAs corresponding to *Mll-Af9* gene in mouse pro-B cell line (wild type cells and 3 clones). A representative gel from 3 independent experiments. Number of circular junctions sequenced for each type of *Mll-Af9* f-circRNAs in mouse pro-B cells (back-spliced, Non canonical back-spliced, and mixed). Sequencing was done from 3 independent experiments. Schemes of f-circRNA-mG and -mH (lower panel) found in the three clones.

FIGURE S1

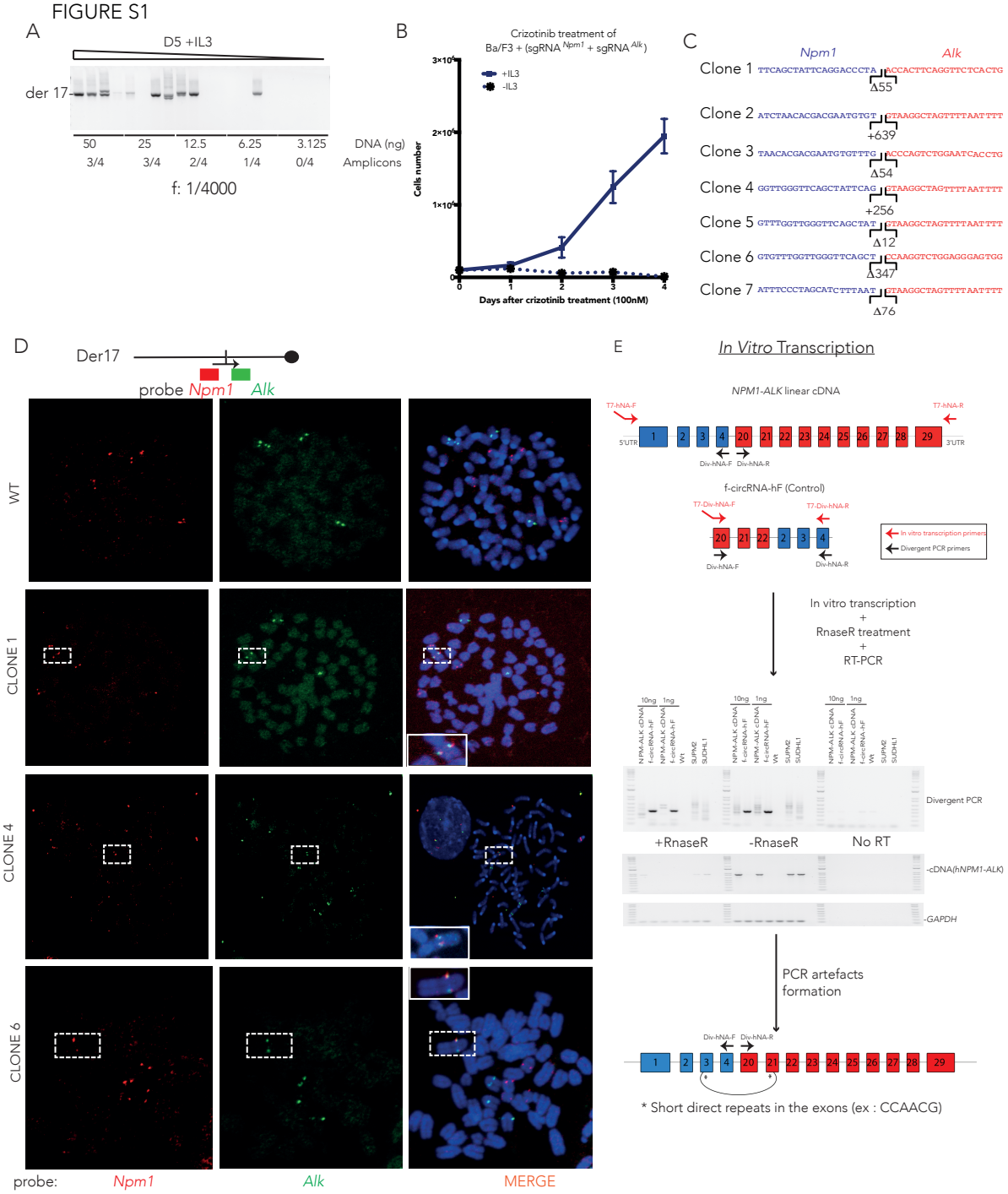
A
D5 +IL3
der 17
50 25 12.5 6.25 3.125
3/4 3/4 2/4 1/4 0/4
DNA (ng)
Amplicons
f: 1/4000
B
Crizotinib treatment of
Ba/F3 + (sgRNA Npm1 + sgRNA Alk)
+IL3
-IL3
Cells number
Days after crizotinib treatment (100nM)
C
Npm1
Alk
Clone 1 TTCAGCTATTCAGGACCCTA ACCACTTCAGGTTCTCACTG Δ55
Clone 2 ATCTAACACGACGAATGTGT GTAAGGCTAGTTTTAATTTT +639
Clone 3 TAACACGACGAATGTGTTTG ACCCAGTCTGGAATCACCTG Δ54
Clone 4 GGTTGGGTTCAGCTATTCAG GTAAGGCTAGTTTTAATTTT +256
Clone 5 GTTTGGTTGGGTTCAGCTAT GTAAGGCTAGTTTTAATTTT Δ12
Clone 6 GTGTTTGGTTGGGTTCAGCT CCAAGGTCTGGAGGGAGTGG Δ347
Clone 7 ATTTCCCTAGCATCTTTAAT GTAAGGCTAGTTTTAATTTT Δ76
D
Der17
probe Npm1 Alk
WT
CLONE 1
CLONE 4
CLONE 6
probe:
Npm1
Alk
MERGE
E
In Vitro Transcription
NPM1-ALK linear cDNA
T7-hNA-F
T7-hNA-R
5'UTR
3'UTR
Div-hNA-F
Div-hNA-R
f-circRNA-hF (Control)
T7-Div-hNA-F
T7-Div-hNA-R
In vitro transcription primers
Divergent PCR primers
In vitro transcription
+
RnaseR treatment
+
RT-PCR
Divergent PCR
+RnaseR
-RnaseR
No RT
-cDNA(hNPM1-ALK)
-GAPDH
PCR artefacts
formation
* Short direct repeats in the exons (ex : CCAACG)

FIGURE S2

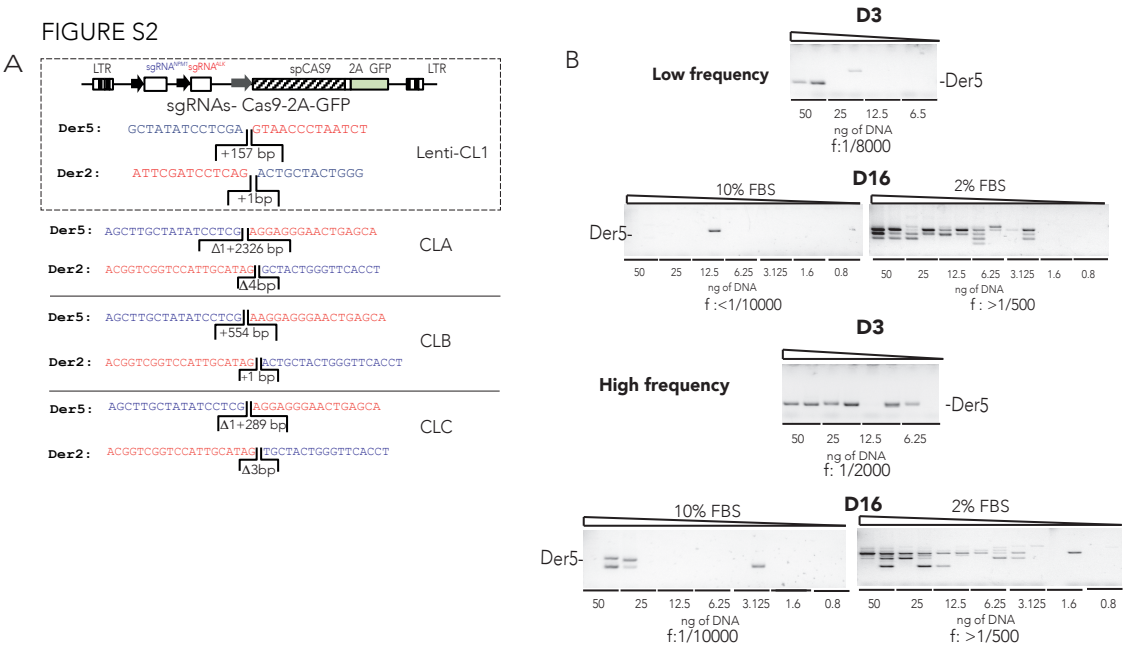
A
LTR
sgRNA
sgRNA
spCAS9
2A GFP
LTR
sgRNAs- Cas9-2A-GFP
Der5: GCTATATCCTCGA GTAACCCTAATCT
+157 bp
Lenti-CL1
Der2: ATTCGATCCTCAG ACTGCTACTGGG
+1bp
Der5: AGCTTGCTATATCCTCG AGGAGGGAACTGAGCA
Δ1+2326 bp
CLA
Der2: ACGGTCGGTCCATTGCATAG GCTACTGGGTTCACCT
Δ4bp
Der5: AGCTTGCTATATCCTCG AAGGAGGGAACTGAGCA
+554 bp
CLB
Der2: ACGGTCGGTCCATTGCATAG ACTGCTACTGGGTTCACCT
+1 bp
Der5: AGCTTGCTATATCCTCG AGGAGGGAACTGAGCA
Δ1+289 bp
CLC
Der2: ACGGTCGGTCCATTGCATAG TGCTACTGGGTTCACCT
Δ3bp

B
D3
Low frequency
-Der5
50 25 12.5 6.5
ng of DNA
f:1/8000
D16
10% FBS
2% FBS
Der5-
50 25 12.5 6.25 3.125 1.6 0.8
ng of DNA
f :<1/10000
f : >1/500
D3
High frequency
-Der5
50 25 12.5 6.25
ng of DNA
f: 1/2000
D16
10% FBS
2% FBS
Der5-
50 25 12.5 6.25 3.125 1.6 0.8
ng of DNA
f:1/10000
f: >1/500

FIGURE S3

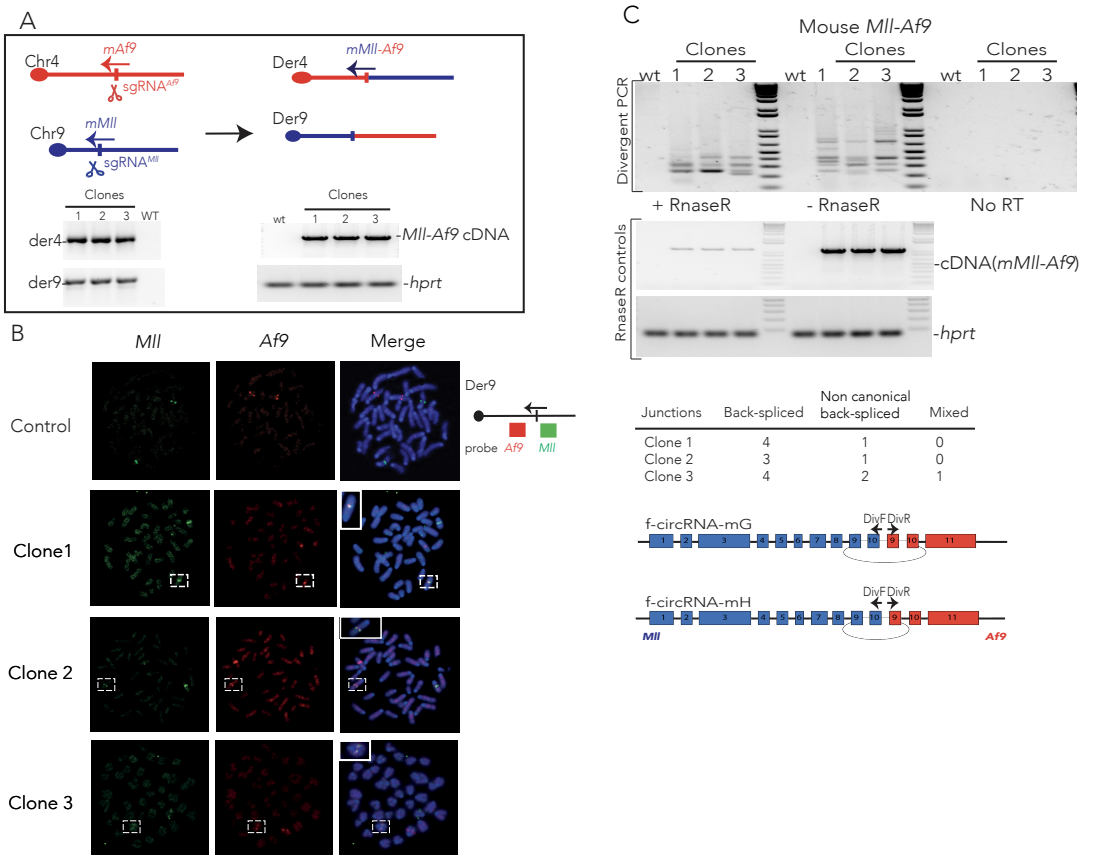

Junctions	Back-spliced	Non canonical back-spliced	Mixed
Clone 1	4	1	0
Clone 2	3	1	0
Clone 3	4	2	1

SUPPLEMENTARY TABLES

Table S1 (Related to Figure 1)
f-circRNAs expressed in mouse *Npm1-Alk* Ba/F3 clones

Schematic representation of f-circRNA junctions obtained from the sequencing of 3 independent experiments. Circularized junctions are linked by a line. Circularization junction sequences of Non-canonical back-spliced and Mixed f-circRNAs are described after each table.

* indicates short repeats.

Sequences mNpm1-Alk circular RNAs :

Clone 2 :

Non canonical back-spliced **:**

ALK Ex 24 AACCCACCTCCCTGGCCATG TGAAATTACACCACCTGTGG Ex 4 NPM

Clone 5 :

Non canonical back-spliced **:**

ALK Ex 23 TGAGTCTACAAGCCCTGCCCCGCTT TCTGTACAACCAACA Ex 3 NPM

Clone 6 :

Non canonical back-spliced **:**

ALK Ex 23 TCATGGCTGGCGGAGACCTC GCGTGATTCCGTCCTGCGCG Ex 1 NPM

Clone 7 :

Non canonical back-spliced **:**

ALK Ex 22 ACGCTGCCAGA CTTTGAAATTACACCACCTGTGGTCTTAC Ex 4 NPM

Table S2 (Related to Figure 3)

f-circRNAs expressed in human *NPM1-ALK* RPE-1 clones, SUDHLI and SUPM2 cells.

Schematic representation of f-circRNA junctions obtained from the sequencing of 3 independent experiments. Circularized junctions are linked by a line. Circularization junction sequences of Non-canonical back-spliced and Mixed f-circRNAs are described after each table.

circular RNAs with the junction in exon 1 corresponding to an identified alternative splice site (ENST00000517671.5)

Sequences hNPM1-ALK circular RNA :

Lenti-CL1, SUDHLI :

Mixed :

ALK Ex 21 CCCTGCAAGTGGCTGTGAAG CGTTCTTTTATCTCCGTCCG Ex 1 NPM

Lenti-CL1 :

Non canonical back-spliced :

ALK Ex 20 CTGGCAAGACCTCCTCCATC TGCACATTGTTGAAGCAGAG Ex 3 NPM

CLB :

Non canonical back-spliced :

ALK Ex 20 GAGGTGCCGCGGAAAAACAT AGCAGAGGCAATGAATTACG Ex 3 NPM

SUDHLI :

Mixed :
ALK Ex 22 ATGGAAGCCCTGATCATCAG CCCCCTGAGGCCCCAGAACT Ex 1 NPM
ALK Ex 20 AAAAACATCACCCTCATTCG CGTTCTTTTATCTCCGTCCG Ex 1 NPM
ALK Ex 20 GGCAAGACCTCCTCCATCAG GTTTCCCTTGGGGGCTTTGA Ex 4 NPM
SUPM2 :
Non canonical back-spliced :
ALK Ex 22 GACGAACTGGATTTCCTCAT TTGAAGCAGAGGCAATGAAT Ex 3 NPM
Mixed :
ALK Ex 20 GACTACAACCCCAACTACTG GTTGTGAACTAAAGGCCGAC Ex 2 NPM
CDNA2 :
Non canonical back-spliced :
ALK Ex 24 CACGTGGCTCGGGACATTGC ACGAAGGCAGTCCAATTAAA Ex 3 NPM

Table S3 (Related to Figure S3)

f-circRNAs expressed in *Mll-Af9* mouse pro-B cells clones

Schematic representation of f-circRNA junctions obtained from the sequencing of 3 independent experiments. Circularized junctions are linked by a line. Circularization junction sequences of Non-canonical back-spliced and Mixed f-circRNAs are described after each table.

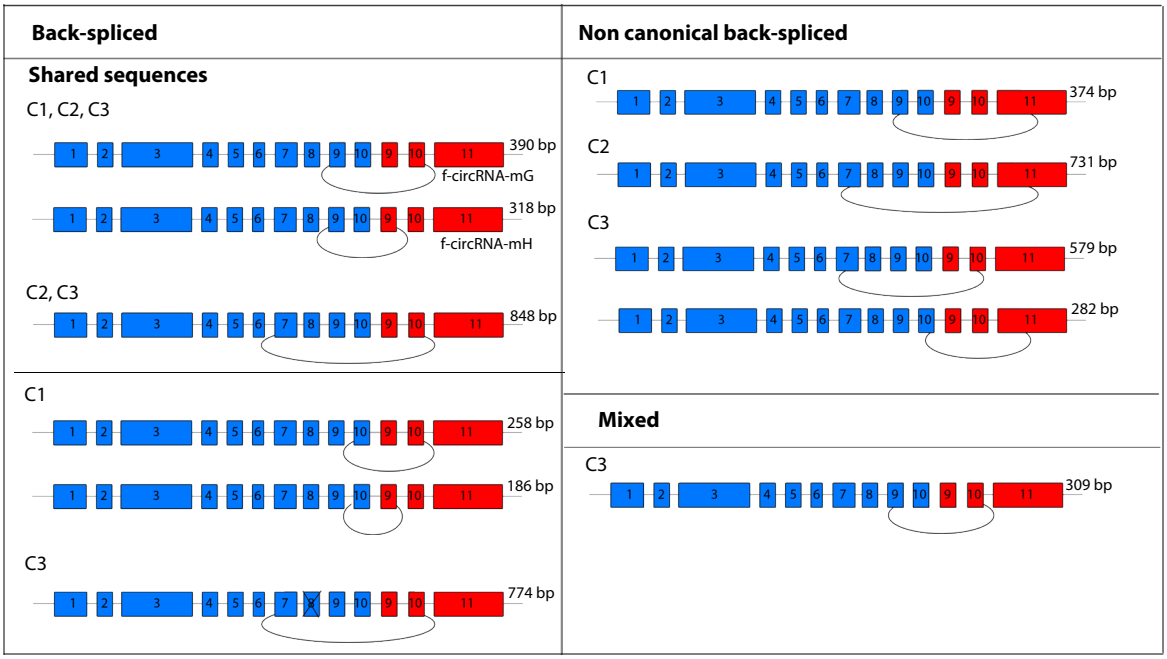

Sequences mMll-Af9 circular RNA

Clone 1 :

Non canonical back-spliced :

AF9 Ex 11 AACCTTATAGAGGAAACTGG TTGAACATCCTCAACCCACT Ex 9 MLL

Clone 2 :

Non canonical back-spliced :

AF9 Ex 11 ACAACAGCTGGACGCATCAA CCAGCAGCCGTCGTCCCCCC Ex 7 MLL

Clone 3 :

Non canonical back-spliced :

AF9 Ex 10 CTGCAGCAGATCGTGAACCT TCCCAGCCAGCAGCCGTCGT Ex 7 MLL

AF9 Ex 11 TTTGCTCGCTGGACAAAACT CCCATAACACCCAGAGTAGT Ex 10 MLL

Mixed :

AF9 Ex 10 GGAACGACACATTCTGCAGC AGTAAACAAGAGAATGCAGG Ex 9 MLL

Table S4 (Related to Transparent Methods)

sgRNA and primer sequences

sgRNA sequences:

Translocation induction
Human NPM1: TAT**CCT**CGAACTGCTAC*TGG*GTTCACCTCAGC
sgRNA^{NPM} 5′-GTGAACCCAGTAGCAGTTCG-3′
Human ALK: GAT**CCT**CAGGTAACCCTAATCTGATCACGGTC
sgRNA^{ALK} 5′-GATCAGATTAGGGTTACCTG-3′
Mouse NPM1: GGA**CCC**TATGACCAATGAGGCTATCTTTCAAT
sgRNA^{NPM} 5′-AGATAGCCTCATTGGTCATA-3′
Mouse ALK: ATAAAATCCTGGCATGTCTATCTGTA**AGG**CTA
sgRNA^{ALK} 5′-TCCTGGCATGTCTATCTGTA-3′
Mouse MLL : CAC**CCC**ACATCCGGTGGTTCACTGTAACTCCA
sgRNA^{MLL} 5′-TACAGTGAACCACCGGATGT-3′
Mouse AF9 : TCT**CCA**TACTCGTTGACTGGTCTATCAGTTTA
sgRNA^{AF9} 5′-GATAGACCAGTCAACGAGTA -3′

Primer sequences:

Plasmid cloning		
Cloning of sgRNA^{NPM}:sgRNA^{ALK}:Cas9-GFP	sgRNA_EE_F	AGGAACCAATgaattcGACTGGATCCGGTACCAAGG
	sgRNA_EE_R	TAGAGAGGTAgaattcAGCGGCCCAAGCTTAAAAA
Cloning of NPM1-ALK cDNA	cDNA_NA _F	CTAAGTGCGgctagcgccaccATGGAAGATTCGATGGACATGG
	cDNA_NA _R	ATAAAAACCTgaattcACCACATCTGGGCCTTGTAT
PCR for translocation detection		
hNPM1-ALK (PCR1)	hNA-Der5-F	CAGTTGCTTGGTTCCCAGTT
	hNA-Der5-R	AGGAATTGGCCTGCCTTAGT
hNPM1-ALK (PCR2)	hNA-Der5-NF	GGGGAGAGGAAATCTTGCTG
	hNA-Der5-NR	GCAGCTTCAGTGCAATCACA
hALK-NPM1 (PCR1)	hAN-Der2-F	TCCTTCAGTGTCCATCACGA
	hAN-Der2-R	GAACCTTGCTACCACCTCCA
hALK-NPM1 (PCR2)	hAN-Der2-NF	CCCACCCCTAGACGTCACT
	hAN-Der2-NR	TTCACATCCTCCTCCTCTTCA
mNPM1-ALK (PCR1)	mNA-Der17-F	CATCGTAGAGGCAGAAGCAA

	mNA-Der17-R	TGCAGTTCCATCTGCATAGC
mNPM1-ALK (PCR2)	mNA-Der17-NF	AGGTCTCTTGCGTCATTTGG
	mNA-Der17-NR	CAGATAGGTGTCCGCTGTGA
mALK-NPM1 (PCR1)	mAN-Der11-F	CTTCAGTGCCCAACACAATG
	mAN-Der11-R	CTTTCCTGGCACACACCTTT
mALK-NPM1 (PCR2)	mAN-Der11-NF	TGGCTCAAGCCATACTAGCC
	mAN-Der11-NR	AGAGGCAGGTGGATTTCTGA
mMLL-AF9 (PCR1)	mMA-Der9-F	TTTTGGGTGAGTTGTTTGGA
	mMA-Der9-R	CAGCGGACAGTTCTGTGGTA
mMLL-AF9 (PCR2)	mMA-Der9-NF	ACACACCAGAAGAGGGCATC
	mMA-Der9-NR	ACCTGCAAAGGTTCTTGTGG
mAF9-MLL (PCR1)	mAM-Der4-F	CAGTGCACCCTTGAGCATAA
	mAM-Der4-R	TAGTCACCAGGCATTTGCAG
mAF9-MLL (PCR2)	mAM-Der4-NF	ACAACTGGCATGTGCAACTC
	mAM-Der4-NR	TGCTAGGGATTGAAGCCAAG

RT-PCR		
hNPM1-ALK cDNA	hRNA-NA-F	TTGTGAACTAAAGGCCGACAAA
	hRNA-NA-R	CAGTTTCTGGCAGCAATGTCTC
mNPM1-ALK cDNA	mRNA-NA-F	GTGGAACAGGAGGCAGTTGT
	mRNA-NA-R	GCAATATCCCGGTGGATAAA
mMLL-AF9 cDNA	mRNA-MA-F	CCTGAACCCAAACAGGTCAG
	mRNA-MA-R	TGGAATGAACCACCACAGAA
hGAPDH cDNA	hGAPDH-F	GCCATCAATGACCCCTTCAT
	hGAPDH-R	TGACAAGCTTCCCGTTCTCA
mHPRT cDNA	mHPRT-F	GCAGTACAGCCCCAAAATGG
	mHPRT-R	GGTCCTTTTCACCAGCAAGCT

PCR for fusion circular RNA detection		
hNPM1-ALK	hNA-div-F	AAGCACCAGGAGCTGCAAG
	hNA-div-R	AATATGCACTGGCCCTGAAC
mNPM1-ALK	mNA-div-F	ACCAGGAGTTGCAGGCTATG
	mNA-div-R	AGATGCTGTCCACTAATGTGC
mMLL-AF9	mMA-div-F	TCCAATAAAACAAAGCAAATCAGA
	mMA-div-R	CACTGCTGGCACAGAGAAAG

PCR for specific fusion circular RNA detection		
f-circRNA-mA	f-circ-mA-F	GCAGGCTATGCAGATGGAAC
	f-circ-mA-R	AGCCTTTAGTTCACAGCCTGA
f-circRNA-mB	f-circ-mB-F	GTCGGAAGCACCAGGAGTT
	f-circ-mB-R	GCCTTTAGTTCACAGCCGG
f-circRNA-hC	f-circ-hC-F	GAGCTGCAGAGCCCTGAGTA
	f-circ-hC-R	GCCTTTAGTTCACAACCGGG
f-circRNA-hD	f-circ-hD-F	AGCACCAGGAGCTGCAAG
	f-circ-hD-R	GGCCTTTAGTTCACAACCTGA
f-circRNA-hE	f-circ-hE-F	GAGCTGCAGAGCCCTGAGTA

	f-circ-hE-R	CCCCCAAGGGAAACCTGA
f-circRNA-hF	f-circ-hF-F	GAGCTGCAGAGCCCTGAGTA
	f-circ-hF-R	CCCCCAAGGGAAACCGGT
PCR for digital droplet PCR		
hGAPDH	GAPDH-F	GCCATCAATGACCCCTTCAT
	GAPDH-R	TGACAAGCTTCCCGTTCTCA
hNPM-ALK	hNA-F	ACCACCAGTGGTCTTAAGGTTG
	hNA-R	CGGAGCTTGCTCAGCTTGTA
PCR for in vitro transcription		
T7-hNPM-ALK	T7-hNA-F	gaaattaatacgactcactata**GGG**GTTCTCTGGAGCAGCGTTCT
	T7-hNA-R	CACATCAACAAGGCAAGGAA
T7-Div-hNA	T7-Div-hNA-F	gaaattaatacgactcactata**GGG**AAGCACCAGGAGCTGCAAG
	T7-Div-hNA-R	AATATGCACTGGCCCTGAAC

TRANSPARENT METHODS

CRISPR/Cas9 plasmids

The sgRNAs vectors were cloned in MLM3636 plasmid (Addgene plasmid 43860). sgRNAs sequences are listed above. SgRNAs targeting human *NPM1* and *ALK* genes have been previously described (Ghezraoui et al., 2014; Renouf et al., 2014). All sgRNAs were designed using the CRISPOR designer tool (http://crispor.tefor.net/crispor.py) and are described in Table S4. Cas9-2A-GFP was expressed from pCas9-GFP vector (Addgene plasmid 44719).
For construction of lentiviral plasmid expressing both sgRNAs, human sgRNA^{NPM1} was firstly cloned in the sgRNA:Cas9-GFP vector from Ebert's laboratory (Heckl et al., 2014). The U6-sgRNA^{ALK} cassette was PCR amplified from MLM3636 vector containing sgRNA^{ALK} and cloned in the EcoRI site of the sgRNA^{NPM1}:Cas9-GFP vector. Lentiviral construct was co-transfected with pCMV 8.74 packaging plasmid, and pMD2.G VSV envelope expression plasmid. Supernatants were collected at 48h and concentrated by ultra-centrifugation.

Cell culture and transfection

The Ba/F3 murine pro-B cell line (gift from Dr F.Meggetto) was cultured in RPMI-1640 medium supplemented with 10% FBS and 5 ng/mL murine recombinant IL-3 (Thermo Fisher Scientific). The SUDHL1 ALCL cell line was cultured in RPMI-1640 medium supplemented with 10% FBS. The SUPM2 ALCL cell line was cultured in RPMI-1640 medium supplemented with 20% FBS. The RPE-1 hTERT-immortalized retinal cell line was cultured in DMEM/F-12 medium supplemented with 10% or 2% FBS. The mouse v-Abl proB-cell line was cultured in RPMI-1640 medium supplemented with 10% FBS, beta-mercaptoethanol (50nM), penicillin and streptomycin (Lescale et al., 2016). (Mediums and FBS from Gibco)
Typically, $1x10^6$ cells were transfected using Nucleofection (Amaxa technology II (Lonza)) with 3 µg of pCas9-GFP vector and 3 µg of each sgRNA, using the Cell Line Nucleofector Kit V (programs D-032 for Ba/F3 and X-001 for RPE-1 and mouse v-Abl proB-cell line). For lentiviral transduction, $1x10^5$ RPE-1 cells were seeded and transduced with concentrated sgRNA^{NPM1}:sgRNA^{ALK}:Cas9-GFP supernatant. Cells were FACS sorted based on GFP expression 72h post-transduction.

IL-3 removal and crizotinib treatment

5 days after transfection of pCas9-2A-GFP and sgRNA^{NPM1}, sgRNA^{ALK}, or both sgRNAs in Ba/F3 cell line, 10^5 cells were cultured without IL-3. Surviving cells were counted every 3

days. IL-3 starved and wild-type Ba/F3 cells were then seeded at 10^5 cells per well in a 6-well plate. Cells were cultured with addition of 100 nM crizotinib (SelleckChem) in medium and counted every days.

PCR-based detection of translocation junctions and translocation frequency

Genomic DNA from cells was extracted using E.Z.N.A Tissue DNA Kit (Omega Biotek). For detection of translocation junctions from pooled cells expressing CRISPR/Cas9, we performed a nested PCR on 50 ng of genomic DNA as previously described (Ghezraoui et al., 2014; Piganeau et al., 2016; Renouf et al., 2014). Primers sequences are listed in Table S4.

Translocation frequency was estimated by serial dilution as previously described (Ghezraoui et al., 2014; Renouf et al., 2014). Briefly one-round PCR was performed on four serial dilutions of DNA from transfected cells, using primers from PCR2.

RT-PCR and cDNA amplification of fusion transcript

5 days after transfection, RNA was extracted using Nucleospin RNA Kit (Macherey Nagel). RT-PCR was performed using ProtoScript® II First Strand cDNA Synthesis Kit (NEB) according to manufacturer's instructions. Primers sequences are listed in Table S4.

***NPM1-ALK* cDNA overexpression**

NPM1-ALK cDNA was amplified by PCR from SUDHLI cells using primers containing NheI and EcoRI sites. PCR product was cloned between NheI and EcoRI sites in pLJM1-EGFP plasmid (Addgene Plasmid 19319). pLJM1-NPM1-ALK vector was then transfected in RPE-1 cells. 24h after transfection 12 µg/ml puromycin was added in the medium. *NPM1-ALK* cDNA expression was assessed by RT-PCR after 2 weeks of selection. Two positive clones were then isolated.

Cloning of translocated cells

Cloning of cytokine-independent Ba/F3 cells was performed by seeding 0.3 cell per well in a 96-well plate. Cloning of translocated RPE-1 cells was performed by sib selection. Pooled cells were seeded in a 96-well plate, at 10^3 cells per well. At confluence, plates were duplicated for translocation detection by PCR screen. One plate was maintained in culture. Cells from the other plate were incubated with lysis buffer (10 mM Tris–HCl pH 8, 0.45 % NP40, 0.45 %Tween20, 100 µg/mL Proteinase K) for 1 hour at 55°C. Proteinase K was inactivated by heating at 95°C for 10 minutes. First-round PCR was performed on lysate with

primers used for translocation junction detection (listed below). Second-round PCR was performed with SYBR green in real-time PCR conditions (Mx3005p, Agilent) (Brunet et al., 2009; Ghezraoui et al., 2014; Renouf et al., 2014). Ba/F3 cells from the remaining plate corresponding to positive wells were amplified in cell culture. RPE-1 cells from remaining plate corresponding to positive wells were re-seeded for additional steps of selection to obtain translocated clones. Of note, cloning of RPE-1 clones A, B and C was performed by seeding 0.3 cell per well (in a 96-well plate) directly after 2 weeks of growth in 2% FBS medium.

Western-blot

Whole cell extracts were prepared with protein lysis buffer (50 mM Tris-HCl at pH 7.4, 1%Triton X-100, 0.1% SDS, 150 mM NaCl, 1 mM EDTA, and 1 mM DTT prepared from a 1 M DTT stock), with addition of Complete cocktail protease inhibitor tablets (Roche) and Halt Protease and Phosphatase Inhibitor Cocktail (Thermo Fisher Scientific). Typically, 30 µg of protein extracts were run on an 8% (w/v) Tris-HCl SDS PAGE gel. For SUDHL1 control cell line, 10 µg of protein extract were used. Gel was blotted, and probed with Phospho-ALK (Tyr1604), ALK (31F12), Phospho-STAT3 (Tyr705), Stat3, Phospho-p44/42 MAPK (ERK1/2) (Thr202/Tyr204), p44/42 MAPK (ERK1/2), Phospho-AKT (Thr308), Phospho-AKT (Ser473), and AKT antibodies from Cell Signaling. Murine NPM1-ALK protein expression was assessed with ALK (M19) antibody (Santa Cruz), and Cas9 with Cas9 (7A9-3A3) antibody (Novus). Alpha-Tubulin mouse antibody (Sigma-Aldrich) was used) as a loading control. Phospho-ALK and Phospho-STAT3 antibodies were used at 1/200 dilution. Other antibodies were used according to manufacturer's recommendations. Secondary antibodies were HRP-conjugated, and blot developed with ECL prime (GE Healthcare Life).

Fluorescence *in situ* hybridization

FISH was performed on metaphases from translocated clones. Human *ALK* and *NPM1* human genes were labeled using respectively ALK Breakapart LPS 019 probe (Cytocell) and homemade *NPM1* probe from BAC RP11-546B8. Murine *Alk* and *Npm1* genes were labeled using homemade probes from BAC RP23-100F5 and RP23-74P19. *Mll* and *Af9* genes were labeled using homemade probes from BAC RP23-23P9 and RP23-440D4. Metaphase spreading, probe labeling, hybridization, washing and fluorescence detection were performed according to standard procedures. Images were taken with the Zeiss Axio Observer.Z1 system.

Selective advantage in high/low serum medium

Cells were plated at day 0 with 10% Lenti-CL1 GFP-positives and 90% WT RPE-1 GFP-negatives. They were cultured in high serum condition (10% FBS) or low serum condition (2% FBS). After 6 and 14 days cells were analyzed on cytometer to detect GFP enrichment.

Translocation detection in high/low serum medium

72 hours after transfection with pCas9-GFP and sgRNA^{ALK} + sgRNA^{NPM1}, cells were cultured in 10% FBS or 2% FBS. DNA extraction was performed at day 3 and day 16 after transfection to estimate the frequency of translocation.

RT-PCR and cDNA amplification for detection of circular RNA

RNA was extracted using Nucleospin RNA Kit (Macherey Nagel). 1 µg RNA was treated by 2U RNaseR enzyme (Epicentre) for 20 minutes at 37°C. RT-PCR was performed using ProtoScript® II First Strand cDNA Synthesis Kit (NEB) according to manufacturer's instructions. cDNA was then PCR amplified. PCR products were cloned directly with TOPO TA cloning kit (ThermoFischer) according to manufacturer's instructions and sequenced by Sanger Sequencing using T7 primer.

***In vitro* transcription assay (Figure S1E)**

Linear *NPM1-ALK* cDNA was amplified from SUPM2 using primers located in 5' and 3' UTR of mRNA (see TABLE S4 for primers sequences). The 5' primer contained the T7 promoter sequence (GAAATTAATACGACTCACTATAGGG) upstream from the specific 5'UTR sequence. Similarly, f-circRNA-hF was amplified (from a TOPO TA clone) using an upstream primer containing the T7 promoter sequence and used as control for circular RNA amplification. *In vitro* transcription was performed using HiScribe T7 High Yield RNA Synthesis Kit (NEB) according to manufacturer's instructions. Purity and size of RNA were assessed by RNA ScreenTape (Agilent, data not shown). Then 10 ng or 1 ng of transcribed RNA was mixed with 1 μg of total RNA from wild type RPE-1 cell line. RNaseR treatment and RT-PCR were performed on the mix as described previously: PCR amplification was done with primers hNA-div-F/R, hRNA-NA-F/R, hGAPDH-F/R (as control).

cDNA amplification for detection of specific circular RNAs for *NPM1-ALK*

A nested PCR was performed on cDNA to specifically amplify back-spliced f-circRNA identified after TOPO TA sequencing. The first round PCR was performed with divergent

primers for 23 cycles. The second round was performed with a forward primer in exon 20 of *Alk* gene and a reverse primer overlapping the circularization junction specific for each f-circRNA (40 cycles, See Supplementary Material for primers sequences). For specific quantification of f-circRNA-hC and –hD, the second round was performed using digital droplet PCR (Biorad) with Evagreen (according to manufacturer's instructions). Primers sequences are listed in Table S4.

NPM1-ALK expression quantification using digital droplet PCR

Quantification of *NPM1-ALK* expression was performed using digital droplet PCR (Biorad) with Evagreen (according to manufacturer's instructions). Normalization was done using *GAPDH* amplification (See below for primers sequences). Primers sequences are listed in Table S4.

RnaseR efficiency

NPM1-ALK fusion cDNA, *GAPDH* cDNA and f-circRNA-hC/-hD were quantified with or without RnaseR treatment using digital droplet PCR (Biorad, See Supplementary Material for primers sequences). RnaseR efficiency was assess as follow:

$$Fold\ enrichment = \frac{\frac{circular\ RNA\ (+RnaseR)}{circular\ RNA\ (-RnaseR)}}{\frac{linear\ RNA(+RnaseR)}{linear\ RNA\ (-RnaseR)}}$$